

## Use Authorization

In presenting this thesis in partial fulfillment of the requirements for an advanced degree at Idaho State University, I agree that the Library shall make it freely available for inspection. I further state that permission to download and/or print my thesis for scholarly purposes may be granted by the Dean of the Graduate School, Dean of my academic division, or by the University Librarian. It is understood that any copying or publication of this thesis for financial gain shall not be allowed without my written permission.

Signature \_\_\_\_\_

Date \_\_\_\_\_

ASSESSMENT OF  $^{137}\text{Cs}$  TO  $^{90}\text{Sr}$  RATIO IN SELECTED SOILS AROUND IDAHO  
NATIONAL LABORATORY

by

Johnson Aina

A thesis

Submitted in partial fulfillment

of the requirements for the degree of

Master of Science in Department of Nuclear Engineering and Health Physics

Idaho State University

Fall 2023

To the Graduate Faculty:

The members of the committee appointed to examine the thesis of Johnson Aina find it satisfactory and recommend that it be accepted.

---

Dr, Richard Brey  
Major Advisor

---

Dr. Dewayne Derryberry  
Committee Member

---

Dr. Rene Rodriguez  
Graduate Faculty Representative

## **Acknowledgements**

It is with heartfelt gratitude that I acknowledge those who have contributed in one way or the other and offer their valuable time and resources to assist me in the completion of this thesis. This thesis would not have been completed without the immense support and guidance of my committee members, help from my friends, and support from my family.

Special thanks to Roy Dunker for providing all the necessary support, advice, and close supervision of my thesis. His knowledge, patience and encouragement were instrumental in the completion of this study. I would also like to express my gratitude to Dr. Richard Brey for his encouragement and painstakingness in reading through and providing technical support for the completion of this study. I would also like to thank Dr. Dewayne Derryberry for providing great insights on the statistical evaluation of my results and walking me through my hypothesis. My sincere thanks also go to Dr. Rene Rodriguez for not only being my Graduate Faculty Representative for my thesis but for his patience in listening to me and providing support to get some chemicals from the Chemistry Department.

I am also thankful for the gift of friends, for their encouragement and their prayers. My sincere thanks to Blaine Gustafson for his immense support throughout my stay in Pocatello.

Words cannot describe the great support of my brother, Peter Aina for his sincere love and concern throughout this journey. I am also grateful for my mom for her prayers, care, and encouragement. My sincere gratitude to my brothers in Christ (Ayokunle Hodonu and Emmanuel Osei) for their immense support in the ministry.

## Table of Contents

List of Figures .....	vii
List of Tables .....	viii
List of Abbreviations and Acronyms .....	ix
Abstract .....	x
Chapter 1 : Introduction .....	1
1.1. Background .....	1
1.2. Aim.....	4
1.3. Hypothesis.....	4
1.3.1. Hypothesis Testing.....	5
1.4. Study site.....	5
Chapter 2 : Literature Review.....	9
2.1. Radioactive fallout .....	9
2.2. Fission products.....	9
2.2.1. Cesium-137.....	10
2.2.2. Strontium-90.....	11
2.3. Cesium-137 and Strontium-90 in the environment .....	12
2.3.1. Cesium-137 in soil and vegetation .....	13
2.3.2. Measurement of <sup>137</sup> Cs in environmental samples.....	14
2.4. Strontium-90 in soil and vegetation .....	15

2.4.1. Strontium-90 analysis in environmental samples .....	15
2.5. Techniques in purification of <sup>90</sup> Sr .....	17
2.5.1. Precipitation/Co-precipitation .....	17
2.5.2. Liquid-liquid extraction (LLE) .....	17
2.5.3. Ion exchange chromatography.....	18
2.5.4. Adsorption .....	18
2.5.5. Electrosorption.....	19
2.5.6. Extraction chromatography (EC).....	19
2.6. Measurement of <sup>90</sup> Sr in environmental samples .....	22
2.6.1. Liquid scintillation counting (LSC).....	23
2.6.2. Cerenkov counting.....	23
2.6.3. Triple-to-double coincidence ratio (TDCR) .....	25
Chapter 3 : Methodology .....	27
3.1. Chemicals and materials.....	27
3.2. Instrumentation and software .....	27
3.3. Sample procedures .....	28
3.4. Sample collection .....	29
3.4.1. Data quality objective .....	29
3.5. Sample preparation.....	32
3.6. Strontium separation .....	32

3.7. Validation of analytical method .....	35
3.8. Strontium measurement.....	36
3.9. Activity concentration calculation .....	36
3.10. Detection limit and minimum detectable activity .....	38
3.11. Uncertainty measurement.....	39
3.12. Method validation by certified reference materials.....	40
Chapter 4 : Results And Discussions .....	42
4.1. Activity concentration of <sup>137</sup> Cs in soil samples.....	42
4.2. Activity concentration of <sup>90</sup> Sr in soil samples.....	42
4.3. Comparisons of ASTM and TDCR methods in <sup>90</sup> Sr activity determination.....	45
4.4. Reproducibility evaluation .....	47
4.5. Performance evaluation of reference materials .....	47
4.5.1. Result validation by certified reference materials .....	49
Chapter 5 : Conclusion.....	55
5.1. Summary of results.....	55
5.2. Future work .....	56
References.....	58

## List of Figures

Figure 1.1. Location of Idaho National Laboratory .....	7
Figure 1.2. Mean areal activities of $^{137}\text{Cs}$ in surface soils at INL offsite .....	8
Figure 1.3. Mean areal activities of $^{90}\text{Sr}$ in surface soils at INL offsite .....	8
Figure 2.1. Eichrom's Sr resin extractant .....	21
Figure 2.2. Acid dependency of $k'$ for different ions at 23 to 25°C Sr resin.....	22
Figure 2.3. Diagram of the principle of TDCR system in the Hidex 300 SL .....	25
Figure 3.1. Hidex 300 SL liquid scintillation counter equipped with TDCR technology. ....	28
Figure 3.2. Flowchart of $^{90}\text{Sr}$ separation.....	32
Figure 3.3. Extraction chromatography setup.....	34
Figure 4.1. Relationship between the ASTM and TDCR methods in determining $^{90}\text{Sr}$ activity..	47
Figure 4.2. Relationship between $^{137}\text{Cs}$ and $^{90}\text{Sr}$ for both ASTM and TDCR methods .....	51
Figure 4.3. Relationship between $^{137}\text{Cs}$ to $^{90}\text{Sr}$ ratio in both ASTM and TDCR methods .....	51
Figure 4.4. Box plot of treatments after log transformation .....	54

## List of Tables

Table 4.1. Results of $^{137}\text{Cs}$ analysis in soil samples .....	43
Table 4.2. Results of $^{90}\text{Sr}$ analysis in soil samples .....	44
Table 4.3. Summary statistics of the ASTM and TDCR methods.....	45
Table 4.4. Shapiro-Wilk test on the ASTM and TDCR methods .....	46
Table 4.5. Two-tailed test for percentage difference between ASTM and TDCR methods.....	46
Table 4.6. Reproducibility test.....	48
Table 4.7. Results of $^{90}\text{Sr}$ in certified reference materials .....	48
Table 4.8. Performance evaluation of reference soil samples .....	49
Table 4.9. Radioactivity concentration in $^{90}\text{Sr}$ and $^{137}\text{Cs}$ in soil samples .....	52
Table 4.10. One-sample t-test of $^{137}\text{Cs}$ to $^{90}\text{Sr}$ ratio.....	53
Table 4.11. Summary of transformed data.....	53

## **List of Abbreviations and Acronyms**

ACS	American Chemical Society
ASTM	American Society for Testing and Materials
ESER	Environmental Surveillance Education and Research
EML	Environmental Monitoring Laboratory
EPA	Environmental Protection Agency
FPA	Fission and Activation Products
INL	Idaho National Laboratory
ISO	International Standard Organization
MAPEP	Mixed Analyte Performance Evaluation Program
NCRP	National Council on Radiation Protection and Measurements
PSQ	Principal Study Question
TDCR	Triple to Double Coincidence Ratio

# Assessment of $^{137}\text{Cs}$ to $^{90}\text{Sr}$ Ratio in Selected Soils Around Idaho National Laboratory

Thesis Abstract – Idaho State University (2023)

Fission products such as  $^{90}\text{Sr}$  and  $^{137}\text{Cs}$  present in the environment can be identified by environmental monitoring programs. To unequivocally quantify the activity of  $^{90}\text{Sr}$ , it is necessary to chemically separate the  $^{90}\text{Sr}$  to prevent interference from higher and lower energy peaks. This study aims to evaluate methods sufficiently sensitive for the detection of global fallout signs in soil samples. The activity of  $^{137}\text{Cs}$  was determined using gamma spectrometry system. Extraction chromatographic isolation of  $^{90}\text{Sr}$  on Sr resin was employed on the soil samples, and the activity of  $^{90}\text{Sr}$  was determined by triple-to-double coincidence ratio (TDCR) counting method by Hidex 300 SL and a  $^{90}\text{Sr}$  efficiency standard ASTM method. All the measured values for  $^{137}\text{Cs}$  concentration were less than the recommended federal screening limit for surface soil. The values observed for  $^{90}\text{Sr}$  concentration in the soil samples for the ASTM and TDCR methods showed good comparisons.

Keywords: Cesium-137, Strontium-90, Efficiency, Triple to double coincidence ratio (TDCR), American Society for Testing and Materials (ASTM), Extraction chromatography, Hidex 300 SL.

## Chapter 1 : Introduction

### 1.1. Background

Radionuclides in the environment are a growing concern due to their real and perceived risks to humans, biota, and environmental health. Radionuclides can pose a long-term and increasing risk to both the environment and humans due to their capacity to bioaccumulate. According to reports, natural and man-made radionuclides in soils can travel to other environmental compartments via the food chain, leaching, soil resuspension, and erosion processes (Ahmad et al., 2019; González-Delgado and Thakur 2022).

Geological sources including the various radionuclides in the three predominant decay chains, cosmogenically produced materials, and singly occurring radionuclides are the main contributors of natural radioactive materials found in the environment. These materials are taken into the body through the intake of water, food, and air. Absorption of natural occurring radioactive materials, such as those of the uranium radioactive decay series, occurs directly from soils and irrigation water or indirectly by root uptake after it is incorporated into plant structures. Other natural radioactive materials such as the radon progenies ( $^{210}\text{Pb}$  and  $^{210}\text{Po}$ ) are absorbed from the surface air through foliar uptake. Anthropogenic radioactive materials have entered the environment from atmospheric nuclear weapon testing and nuclear accidents. Industrial operations in the military sector, fuel reprocessing, and disposal of nuclear wastes all contribute to the environmental accumulation of radioactive materials (Chaligava et al. 2022; Carvalho et al. 2012; Carvalho et al. 2014).

The radioactive materials in the environment potentially provide dose to humans and other organisms by direct external exposures or by internal radiation exposure after being ingested or inhaled. To assess the harmful effects of radioactive contamination on the environment and human

health, the radionuclides present in environmental samples such as soil, water, vegetation, etc. must be identified (González-Delgado and Thakur 2022). Surveillance and monitoring activities have accumulated a vast database of radioactive materials present in the environment.

The fission product radionuclides  $^{137}\text{Cs}$  and  $^{90}\text{Sr}$  are present in the environment and somewhat ubiquitously identified by both historical and current environmental monitoring and surveillance programs. A large amount of  $^{137}\text{Cs}$  and  $^{90}\text{Sr}$  has been deposited in the environment because of above-ground weapon testing and to a lesser extent nuclear accidents. Due to their moderately long half-lives of 30 and 28.5 years, respectively, and relatively high biological availability, these radionuclides are of particular concern in the environment and may provide negative effects on human health. Other common sources of soil and crop contamination is radioactive airborne emissions. The growing, leafy plants easily take in airborne radionuclides and produce a sizeable fraction of the radiation dose from airborne radioactive effluents (Bondar et al. 2014). Generally, this type of environmental contamination is only happening near time to some nuclear event and to a much lesser degree from resuspension from soil due to fire and or weathering event.

Cesium-137 is a radioactive isotope that can have harmful effects on human health if present in high concentrations in the environment. Risks from  $^{137}\text{Cs}$  vary with its diffusion rates in soil. Cesium tends to recycle within the top 5 cm of soil (Ahmad et al. 2019). Strontium is a chemical congener of calcium and tends to be incorporated into the bone. Bioaccumulation of these radionuclides often starts with root uptake from contaminated soils over long periods of time. This becomes the primary way that Cesium and Strontium enter the human food chain, either directly through the consumption of plant material or indirectly through the consumption of products from animals that have eaten contaminated plant material (Penrose et al. 2015).

After the Fukushima accident, gamma emitting radionuclides such as iodine, tellerium and cesium isotopes were studied. Since gamma rays emanate at discrete energies, qualitative radioisotope identification can be accomplished by examining the energy spectra of gamma rays without element specific separation or laborious sample preparation. Direct field measurement of the radiation from  $^{90}\text{Sr}$  or any beta emitter is virtually impossible. To unequivocally quantify the activity of  $^{90}\text{Sr}$ , it is necessary to chemically separate the  $^{90}\text{Sr}$  to prevent interference from both higher and lower energy peaks (Brennan et al. 2019; Sahoo et al. 2016). There is therefore a desirability of using  $^{137}\text{Cs}$  as a monitor for  $^{90}\text{Sr}$  because  $^{137}\text{Cs}$  emits gamma rays with discrete energy and can be quantified with comparative ease from bulk samples of low specific activity without using the more expensive and time-consuming chemical processes necessary for the measurement of  $^{90}\text{Sr}$  beta emitter (Gustafson 1959; Muck et.al. 2017).

The activity ratio of  $^{137}\text{Cs}$  to  $^{90}\text{Sr}$  from the global fallout deposition has been estimated to be between 1.6 and 1.8 (Miki et al. 2016; Nguyen et al. 2020). According to Sherrill et al. (1975), the ratio of  $^{137}\text{Cs}$  to  $^{90}\text{Sr}$  is approximately unity if they are produced primarily by the fission of  $^{235}\text{U}$ , but greater than 2 if these isotopes are produced by the fission of  $^{239}\text{Pu}$ . In a fission process, approximately 1.76 atoms of  $^{137}\text{Cs}$  are produced for each atom of  $^{90}\text{Sr}$  which leads to a ratio of  $^{137}\text{Cs}$  to  $^{90}\text{Sr}$  of 1.83. This ratio is universally prevalent in fallout if no fractionation occurs from time of detonation to the time of deposition on the ground (Gustafson 1959).

According to the National Institute for Occupational Safety and Health's (NIOSH's) evaluation report for the Argonne National Laboratory West (ANL-W), it was assumed that  $^{137}\text{Cs}$  and  $^{90}\text{Sr}$  can be used to assign dosimetry-significant fission and activation product (FAP) and actinide intakes using the ratio method. These data were analyzed to know if there exist a consistent relationship between the concentration ratio of  $^{137}\text{Cs}$  to  $^{90}\text{Sr}$ , and to determine if these indicating

radionuclides could be used to assign other radionuclide intakes such as FAP for dose reconstruction purposes. However, Sanford Cohen and Associates (SC&A) finds that the measured  $^{137}\text{Cs}$  to  $^{90}\text{Sr}$  ratio values are not sufficiently constant to assume a ratio of unity because 68% of the annual data pairs were greater or less than unity (Buchanan, 2017). Variation of  $^{137}\text{Cs}$  and  $^{90}\text{Sr}$  in the environment reflects the different biological and chemical processes that affect these elements. Over the years, there has been various inconsistencies in the determination of  $^{90}\text{Sr}$ , and lack of information about  $^{137}\text{Cs}$  to  $^{90}\text{Sr}$  concentration ratio in soils and vegetations around INL (INL ESER 2020).

## **1.2. Aim**

Due to the rapid incorporation of  $^{137}\text{Cs}$  and  $^{90}\text{Sr}$  into the food chain, and their long biological half-lives in the human body, it is crucial to regularly monitor these radionuclides in the environmental and in food samples, especially those taken near nuclear facilities. This data may inform decisions on how to best protect people and the environment from radioactive risks (Cao et al. 2021). The aim of this study is to determine the activity concentrations of  $^{137}\text{Cs}$  and  $^{90}\text{Sr}$  in soil samples, to determine contributing factors in the fate and transport of  $^{137}\text{Cs}$  and  $^{90}\text{Sr}$  in environmental samples, and to distinguish between different types of radioactive contamination sources in the environment.

## **1.3. Hypothesis**

$H_{1,0}$ : The ratio of  $^{137}\text{Cs}$  to  $^{90}\text{Sr}$  is equal to the expected value.

$H_{1,a}$ : The ratio of  $^{137}\text{Cs}$  to  $^{90}\text{Sr}$  is not equal to the expected value, indicating that there may be differences in the way these radionuclides are released and transported in the environment.

$H_{2,0}$ : There is no difference between the ratio of  $^{137}\text{Cs}$  to  $^{90}\text{Sr}$  around the INL compared to other areas farther away.

$H_{2,a}$ : The ratio of  $^{137}\text{Cs}$  to  $^{90}\text{Sr}$  around the INL is higher than the ratio of  $^{137}\text{Cs}$  to  $^{90}\text{Sr}$  in other areas due to the nuclear activities of the INL.

$H_{3,0}$ : There is no significant difference between the means of the traditional method (ASTM) used for determining  $^{90}\text{Sr}$  activity concentration and the TDCR method.

$H_{3,a}$ : There is a significant difference between the means of the traditional method (ASTM) used for determining  $^{90}\text{Sr}$  activity concentration and the TDCR method.

### **1.3.1. Hypothesis Testing**

A one-sample t-test was performed to determine whether the observed ratio significantly differs from the expected value. A log transformation was performed to determine if a difference exists between the observed ratio around INL and areas farther away. A two-tailed test was used to determine the difference between the ASTM and TDCR methods used in determining the activity concentration of  $^{90}\text{Sr}$ .

### **1.4. Study site**

The Idaho National Laboratory (INL) site covers about 2,305 km<sup>2</sup> (890 mi<sup>2</sup>) of the upper Snake River Plain in southeastern Idaho at the foot of the Lost River, Lemhi, Beaverhead, and Centennial Mountain ranges. More than 50% of the INL site is located in Butte County while the rest is distributed across Bingham, Bonneville, Clark, and Jefferson counties. The INL site from North to South, extends 63 km (39 mi) and approximately 61 km (38 mi) from east to west. The southeast entrance is approximately 40 km (25 mi) west of Idaho Falls by the highway. Other

towns surrounding the INL site (Figure 1.1) include Arco, Atomic City, Montevideo, Blackfoot, Carey, Dubois, Terreton, and Howe (INL 2020).

Due to global fallout,  $^{137}\text{Cs}$ ,  $^{90}\text{Sr}$ ,  $^{238}\text{Pu}$ ,  $^{239/240}\text{Pu}$ , and  $^{241}\text{Am}$  can be detected in soil throughout the world including on the INL but some of these types of radioactive material may be found in soils of the National laboratory due to INL site operations. These radioactive materials are of particular interest because of their abundance resulting from nuclear fission events such as  $^{137}\text{Cs}$  and  $^{90}\text{Sr}$ , or from their persistence in the environment due to long half-lives such as  $^{238}\text{Pu}$ ,  $^{239/240}\text{Pu}$ , and  $^{241}\text{Am}$ . Analysis of  $^{137}\text{Cs}$  by the Environmental Surveillance, Education and Research (ESER) program from previous years confirmed that the gamma emitting radionuclide remains in the top 5-cm layer of the soil profile. The decay corrected (to half-life value) values of  $^{137}\text{Cs}$  from 1978 to 2020 are presented in Figure 1.2. The values assumed an initial mean areal activity measured in 1978 and a half-life of 30.17 years while the decreasing trend in the mean activity in soil samples was exponential ( $r^2=0.81$ ). Similarly,  $^{90}\text{Sr}$  results according to ESER from 1978 to 2020 are presented in Figure 1.3. The mean annual concentrations of  $^{90}\text{Sr}$  in surface soils decreases at a rate which exceeds that projected for radioactive decay over time. The values assumed an initial mean areal activity measured in 1978 and a half-life of 28.8 years while the decreasing trend in the mean activity in soil samples was a second order polynomial ( $r^2=0.86$ ).

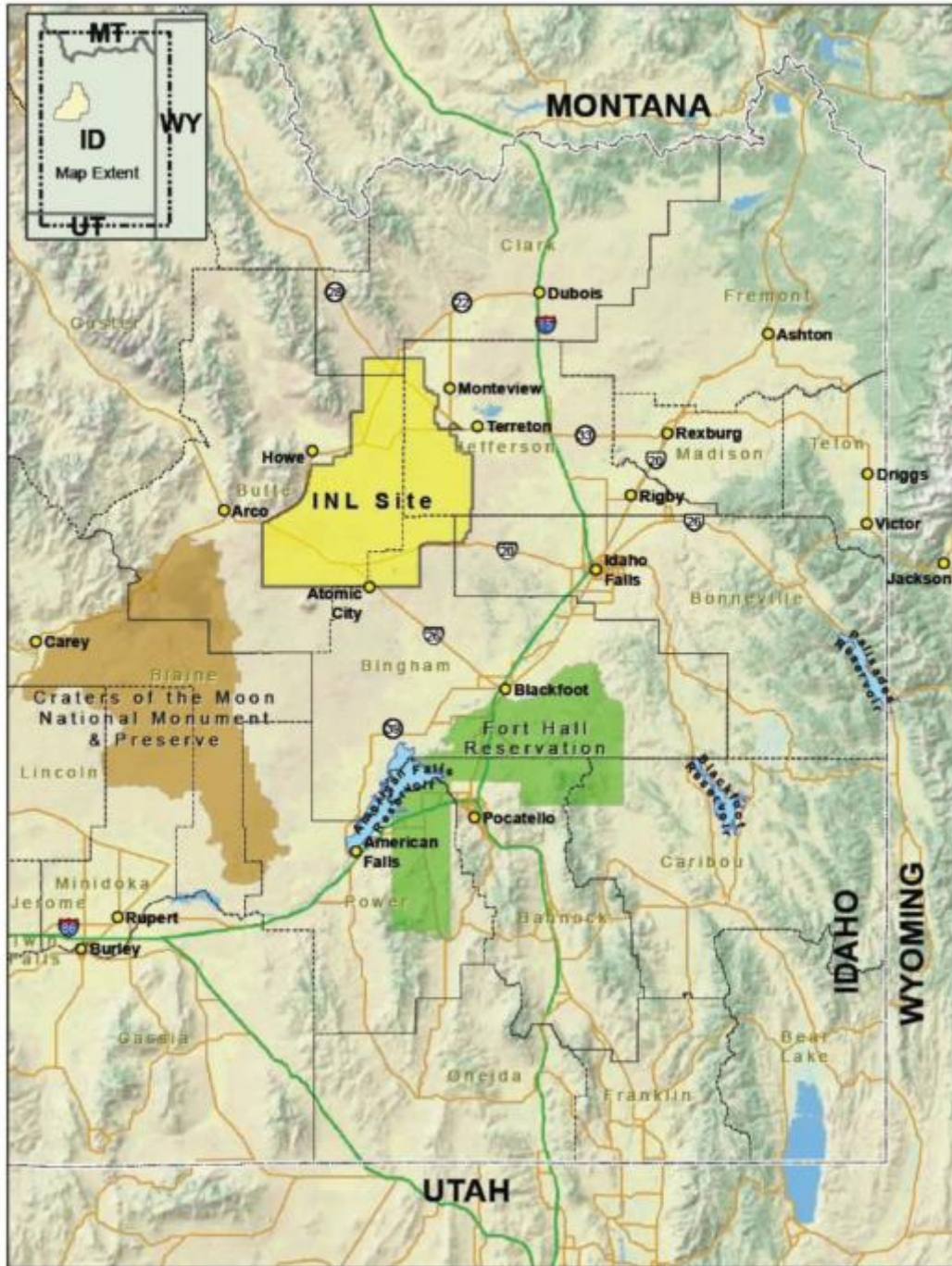


Figure 1.1. Location of Idaho National Laboratory (Source: INL 2020)

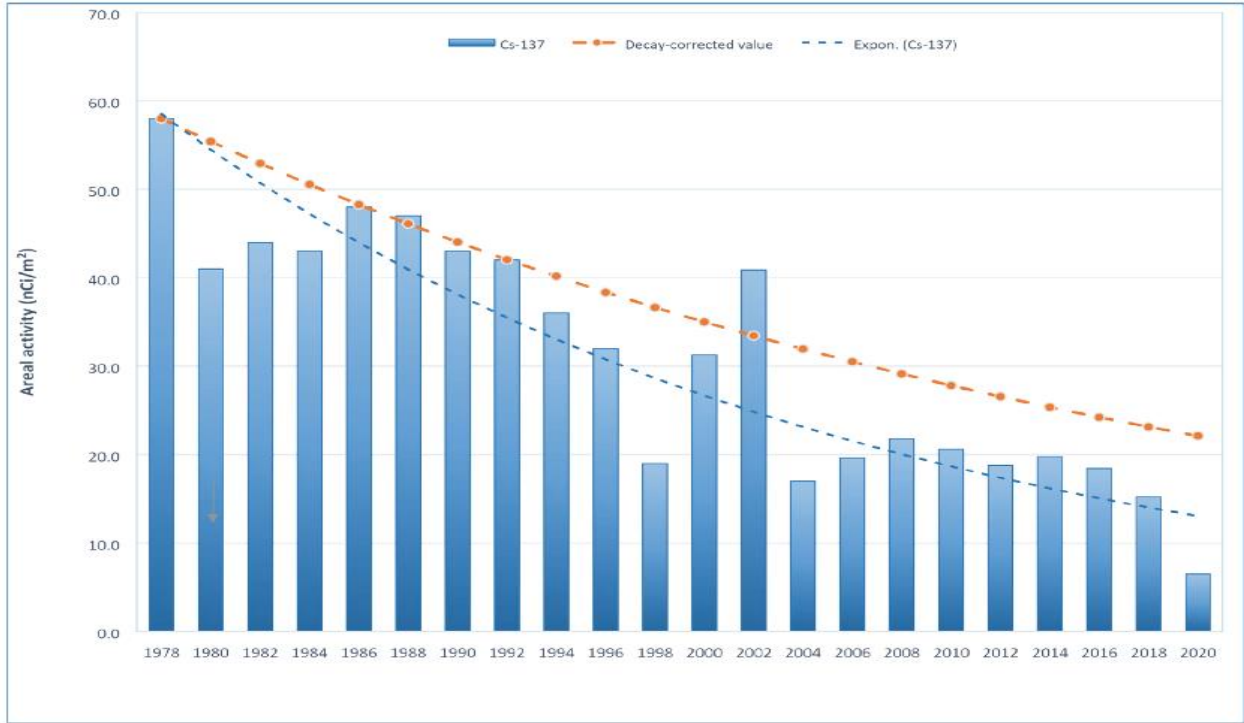


Figure 1.2. Mean areal activities of <sup>137</sup>Cs in surface soils at INL offsite (Source: INL 2020)

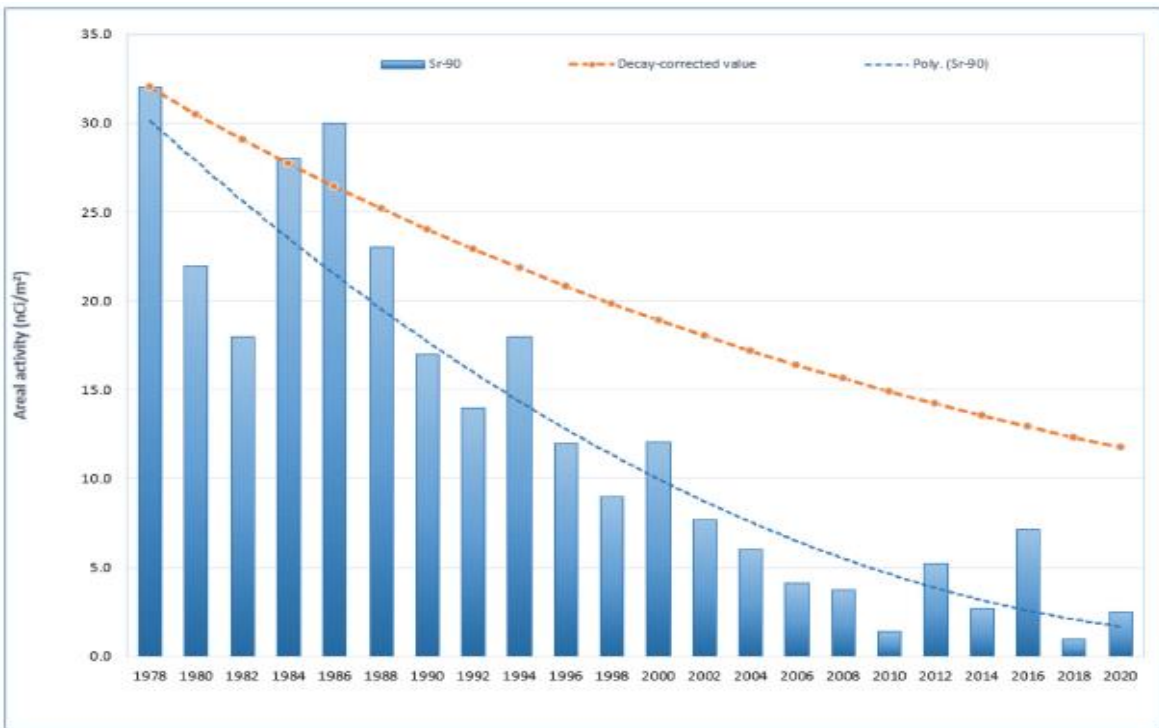


Figure 1.3. Mean areal activities of <sup>90</sup>Sr in surface soils at INL offsite (Source: INL 2020)

## **Chapter 2 : Literature Review**

### **2.1. Radioactive fallout**

Fallout refers to radioactive particles that are carried into the atmosphere after a nuclear accident, nuclear explosion, or atmospheric nuclear testing and gradually falling back as dust or as precipitation (Smith 2018). Fallout consists of fission and activation products, weapon debris and activation radioactive soil in the case of ground explosions. Although some of these particles fall back directly within several minutes after an explosion or accident, some travel high into the atmosphere thereby making them dispersed over the earth after hours, days, months and sometimes years. Deposition, therefore, can occur up to several years after a nuclear weapon detonation depending on particle size and height of a mushroom cloud (Simon et al. 2006).

Generally, the size of fallout particles ranges from a thousandth of an inch to many millimeters. Fallout can be divided into two categories: early fallout, which occurs within the first 24 hours after an explosion, or delayed fallout, which occurs days or years later after the nuclear incident. Radioactive fallout patterns are strongly dependent on the wind speed and direction, and terrain. Rainfall also plays a significant role in deposition since rain can aid in transporting such particles to the surface as washout (Craig et al. 1986).

### **2.2. Fission products**

When a heavy parent nucleus divides into two or more daughter nuclei as a result of nuclear reactions, this phenomenon is called nuclear fission. During the fission process, neutrons interact with a target nucleus creating a compound nucleus that is unstable and then splits into smaller nuclei releasing two or more neutrons, energy, and fission fragments. These fission fragments are individual nuclei, collectively known as fission products. There are about 800 different radionuclide species. Most of them undergo isobaric transitions emitting a series of beta particles

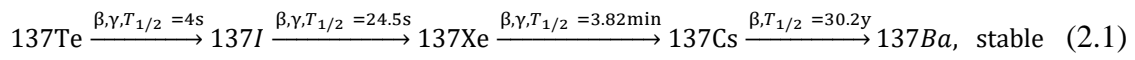
and gamma rays. Many are part of decay chains with progeny having half-lives that generally start out to be short and become longer at the later stages of the chain. As beta particles are released, the atomic number of the isotope increases. The maximum yield of any of the particular fission product is less than 7%. Examples of fission products include Cesium-137, Strontium-90, Krypton-85, Iodine-131, Cerium-144, Technetium-99, among others (Hasan et al. 2014; Murray 2003).

Among the different released fission radionuclides, the two high-yield fission products  $^{137}\text{Cs}$  and  $^{90}\text{Sr}$  are the most significant ones because they contribute to long term doses to population due to their relatively long half-lives (Herranz et al. 2011; Cao et al. 2021). A thorough understanding of the long-term behavior of radionuclides in the environment is necessary to estimate the consequent long-term radiation doses that humans may be exposed to either by exposure to radioactive materials on the ground or through ingestion by food or water (Corcho-Alvarado et al. 2016).

### **2.2.1. Cesium-137**

Cesium is an alkali metal ion that belongs to Group 1 of the periodic table and occurs in the environment as a univalent cation (Lee et al. 2016). Out of the forty known isotopes of cesium,  $^{133}\text{Cs}$  is the only stable isotope.  $^{137}\text{Cs}$ , one of the isotopes of cesium is a fission product of  $^{235}\text{U}$  with its decay chain depicted in equation 2.1. Among the three major isotopes of cesium,  $^{137}\text{Cs}$  and  $^{135}\text{Cs}$  are the fission products while  $^{134}\text{Cs}$  is an activation product (Russell et al. 2015). Cesium-137 and Cesium-135 pose a threat due to their long half-lives (30.2 years and  $3 \times 10^6$  years respectively) and relatively high fission yield of 6.18% and 6.54% respectively. Cesium-137 has a biological behavior similar to potassium. It can be transferred into the human body through the food chain and readily substitutes potassium during transport in the cell membrane (Cao et al. 2022). It undergoes isobaric transition emitting a beta 94.6% ( $E_{\text{max}} = 0.512 \text{ MeV}$ ) to a metastable

barium,  $^{137m}\text{Ba}$  ( $E_{\text{max}} = 514 \text{ keV}$ ,  $t_{1/2} = 2.6 \text{ min}$ ) which in turn decays to a stable state of  $^{137}\text{Ba}$  via isomeric transition emitting a 662 keV gamma photon. About 5.4% of the time,  $^{137}\text{Cs}$  decay directly to stable barium,  $^{137}\text{Ba}$  emitting an energetic beta particle with 1174 keV maximum energy (Mehmood 2018). The latter decay is mostly responsible for the possibility of Cherenkov radiation counting of  $^{137}\text{Cs}$ , with only a minor contribution from the 514 keV beta particle, or internal conversion of the energetic  $^{137m}\text{Ba}$  nucleus as an alternative to the 662 keV gamma photons (Torres et al. 2001).



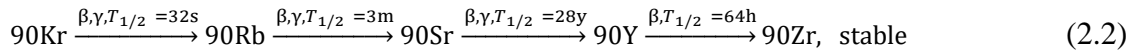
### 2.2.2. Strontium-90

Strontium is an alkali earth metal that belongs to the Group II element. Important radioactive strontium isotopes which occur because of nuclear accidents, above ground nuclear weapon testing, or normal operation of nuclear facilities are  $^{85}\text{Sr}$  ( $t_{1/2} = 64.84 \text{ days}$ ),  $^{89}\text{Sr}$  ( $t_{1/2} = 50.52 \text{ days}$ ), and  $^{90}\text{Sr}$  ( $t_{1/2} = 28.8 \text{ years}$ ). Other radioactive strontium with short half-lives (a few hours) emitting both beta particles and gamma radiation are  $^{91}\text{Sr}$  and  $^{92}\text{Sr}$  (Vajda and Kim 2010; Burger and Lichtsceidl 2019; Sahoo et al. 2016).

Strontium-90 is one of the hazardous by-products of thermal fission of Uranium-235 and Plutonium-239. Its radiotoxicity is due to its long physical half-life of 28.8 years, long biological half-life of 13 years, and high fission yield of 6% (Tayeb et al. 2014; Marchesani et al. 2022). Strontium-90 is also radiotoxic because it is a chemical congener of and has behavior similar to calcium (a typical bone seeking element) as they both belong to group IIA. Strontium can be easily dissolved in water, and thus it's mobile in the environment and can be transported through different

pathways from the environment into the food chain and finally enter the human body (Rivera-Silva et al. 2018; Zhou et al. 2022).

Due to its high chemical reactivity,  $^{90}\text{Sr}$  is typically found in mineral compounds, with celestine ( $\text{SrSO}_4$ ) and strontianite ( $\text{SrCO}_3$ ) being the two basic minerals of strontium.  $^{90}\text{Sr}$  decays to Yttrium-90 ( $t_{1/2} = 64$  hours) by emitting a pure beta particle with maximum beta energy of 546 keV which subsequently decays to Zirconium-90 by emitting an energetic 2280 keV beta particle (Equation 2.2). Typically,  $^{90}\text{Y}$  and  $^{90}\text{Sr}$  are bound to exist in secular equilibrium which damages the bones and bone marrow in which strontium has been incorporated (Mehmood 2018; Marchesani et al. 2022).



### 2.3. Cesium-137 and Strontium-90 in the environment

The nuclear era which began in 1945 with atmospheric nuclear weapon testing (NWT) peaked in the mid 1960's and led to radioactive pollution worldwide. Nuclear accidents such as the Chernobyl accident and Fukushima accident in 1986 and 2011 respectively further deposited radioactive pollutants into the environment. The radionuclides,  $^{137}\text{Cs}$  and  $^{90}\text{Sr}$  play a significant role in the environment due to their assimilation by plants, which animals feed on and finally by human beings (Sarap et al. 2014). This represents a typical concentration effect along the food chain.

The activity ratio of  $^{137}\text{Cs}$  to  $^{90}\text{Sr}$  ( $^{137}\text{Cs}/^{90}\text{Sr}$ ) from the global fallout deposition has been calculated as 1.6:1. Due to higher solubility of  $^{90}\text{Sr}$  compared to  $^{137}\text{Cs}$ , the ratio of  $^{137}\text{Cs}$  to  $^{90}\text{Sr}$  would be expected to increase in the years following the deposition of fallout on soil (Eisenbud and Gesell 1997). The amount of  $^{137}\text{Cs}$  and  $^{90}\text{Sr}$  released because of weapon testing fallout was

calculated to be 960 PBq and 600 PBq respectively (Smith 2018; NCBI 2023). Cesium-137 and Strontium-90 concentrations that have entered the ocean or the marine environment due to radioactive fallout from atmospheric nuclear testing have been reported to be 603 PBq and 377 PBq respectively (Lee et al. 2016; Nguyen et al. 2020). The nuclear accident at Chernobyl released an estimated amount of 10 PBq of  $^{90}\text{Sr}$  and 85 PBq of  $^{137}\text{Cs}$  into the atmosphere while the amount of  $^{90}\text{Sr}$  and  $^{137}\text{Cs}$  released from the Fukushima Daiichi power plant accident have been calculated to be 0.14 PBq and 20 PBq respectively (Miki et al. 2016).

### **2.3.1. Cesium-137 in soil and vegetation**

Cesium-137 can be quickly and strongly absorbed by fine soil particles such as clay minerals and organic matter in topsoil after it reaches the earth's surface by deposition. Strong absorption of  $^{137}\text{Cesium}$  occurs close to the surface in most soils. Once it has been absorbed by the soil, its movement in the soil is limited by chemical processes and its redistribution in landscape is affected by soil movement due to physical processes such as erosion and tillage practice (Andrello and Appoloni 2004). Under several influencing processes (degradation, mechanical removal with rainwater, vertical migration, and diffusion into deeper soil layers) the concentration of  $^{137}\text{Cs}$  in the surface soil drops. The two (not including enhanced transport caused by biological systems) fundamental processes that govern the migration of fallout in undisturbed soil columns are percolation downward with rainwater, and second, the solvable phase is subject to convection and diffusion of any phases within the soil solution and sorption to the soil matter described by the convection-diffusion model equation (Hamzah et al. 2012).

Cesium is tightly bound to soil but does not travel very far below the surface (Eisenbud and Gesell 1997). Consumption of agricultural produce contaminated with radiocesium is the major pathway of human exposure to this radionuclide (Zhu and Smolders 2000). The amount of

$^{137}\text{Cs}$  present in a vegetative ecosystem is first dependent on direct deposition and then the uptake from soil (Bosworth 1995). The extent of accumulation is also dependent on physical and chemical processes of the soil and the plant species (Penrose et al. 2014). Cesium mobility in soils is strongly affected by soil properties such as clay content, organic matter content, potassium content, pH, and ammonium concentration. Cesium shows very low mobility and low availability for plant uptake in soils rich in clay (Corcho-Alvarado et al. 2016).

### **2.3.2. Measurement of $^{137}\text{Cs}$ in environmental samples**

The measurement of  $^{137}\text{Cs}$  requires an extremely high sensitivity due to its low concentration in environmental samples after the era of nuclear weapon testing or major nuclear accidents such as Chernobyl and Fukushima. Cesium-137 can be determined through beta counting or gamma spectrometry. However, gamma spectrometry is commonly used because most samples can be directly counted without the need for chemical separation (Buchtela 2019).

Gamma spectrometry is an analytical method used for the quantification and identification of gamma emitting isotopes in a variety of matrices. The gamma spectrometer consists of an amplifier, pulse amplitude analyzer, preamplifier, high voltage power supply, spectrum data analysis, processing system, etc. Advantages of gamma spectrometer include: 1) fast and convenient, 2) it does not require complex sample separation, and 3) direct measurement of samples due to slight attenuation by the sample matrix. The sample with an appropriate geometric shape is placed in the certain position of the germanium spectrometer system (or sodium iodide), and the gamma ray spectrum is obtained to locate the position of the full-energy peak, net peak area, gamma ray emission probability, sample volume or mass, and other related parameters to determine the type of radionuclide and specific activity contained in the sample (Cao et al. 2022).

## **2.4. Strontium-90 in soil and vegetation**

Strontium contamination in soil is often caused by direct anthropogenic source deposition. It can also be caused by geogenic processes such as bedrock weathering and leaching that may redistribute it within the biosphere. The food chain is the main route by which environmental strontium enters the human body. Strontium contamination in soil is further absorbed by the plant roots and translocated to other parts of the plants aboveground. This absorption is dependent on soil acidity, climatic conditions, and root depth. These plants with  $^{90}\text{Sr}$  upon harvesting may be assimilated in the food cycle and further bioaccumulate in humans and animals. Thus, the ingestion of  $^{90}\text{Sr}$  through contaminated water and food is an important exposure pathway for the population (Sharma 2020).

Plants absorb radioactive fallout deposited on soil from atmospheric emissions or via irrigation using contaminated water sources. Strontium penetrates plants either by foliar absorption or root uptake from soil and water. It may also be taken up by leaves from air, especially in varying degrees after fallout events. The contamination progresses through trophic levels to animals. The radiological impact of strontium released to the environment is usually quantified by mathematical model coefficients referred to as soil-to-plant transfer factors (TF) and plant-to-animal transfer coefficients (TC) (Brennan et al. 2019; Burger and Lichtscheidl 2019; Sharma 2020).

### **2.4.1. Strontium-90 analysis in environmental samples**

It is much easier to measure gamma radiation than to measure beta emitters particularly when emissions are associated with pure beta emissions. The energy distribution of the emitted electrons in the beta decay is continuous, therefore element specific separation from the interfering beta emitters is necessary for qualitative radionuclide identification. This makes  $^{90}\text{Sr}$  determination a complicated, time-consuming procedure requiring corrosive and aggressive chemicals during

sample preparation (Sahoo et al. 2016). The major problem associated with strontium measurement is the separation of Sr from alkaline earth radionuclides such as  $^{133}\text{Ba}$ ,  $^{140}\text{Ba}$ ,  $^{226}\text{Ra}$ ,  $^{228}\text{Ra}$ , alkaline earth matrix components and several other interferences such as Pb and Y nuclides (Vajda and Kim 2010).

Generally, analytical procedures for  $^{90}\text{Sr}$  determination are divided into three stages including sample pretreatment, chemical separation/purification, and measurement. Sample pretreatment objectives are to obtain homogeneous sample solutions that contains the analytes, pre-concentrating the analyte- which involves the removal of insoluble residues that would interfere during the subsequent chemical processing and removing the majority of any sample matrix such as organic matter and stable strontium (both from sample and carrier) (Vajda and Kim 2010, Zhou et al. 2022).

The selection of a sample pretreatment method depends on the sample type. The pretreatment of solid environmental samples such as soil, sediment, atmospheric particles, etc. are similar, and generally include drying, ashing and digestion. Three digestion methods are usually applied to environmental samples, they include acid digestion which requires less expensive equipment and materials. A second method is microwave digestion. This is highly efficient, and it's characterized by its digestion speed, the need for small amount of acid and its small amount of sample consumption. The third digestion technique commonly used is called fusion which is a more rapid, total decomposition that requires ultra-high temperature ( $600^{\circ}\text{C}$ ) (Shao et al. 2018).

The major purpose of chemical purification is to remove interferences from target radionuclides in order to obtain a purified fraction. Chemical purification involves precipitation, calcination, acid, and alkali treatment, leaching, etc. Interferences in measurements of  $^{90}\text{Sr}$  or  $^{90}\text{Y}$

with radiometric methods include any and all other beta emitters which directly affects the detection of  $^{90}\text{Sr}$  and any alpha or gamma emitters which increases the background.

## **2.5. Techniques in purification of $^{90}\text{Sr}$**

Different techniques have been employed for chemical separation and purification of  $^{90}\text{Sr}$ . Such techniques include precipitation/co-precipitation, liquid-liquid extraction, ion-exchange chromatography, extraction chromatography, electrosorption and adsorption (Vajda and Kim 2010, Zhou et al. 2022).

### **2.5.1. Precipitation/Co-precipitation**

This technique is the oldest and most widely method used for  $^{90}\text{Sr}$  purification. It involves nitrate precipitation using fuming nitric acid. To achieve the selective isolation of  $^{90}\text{Sr}$ , this method uses a low solubility of  $\text{Sr}(\text{NO}_3)_2$  in a high concentration (typically  $>14\text{ M}$ ) of nitric acid (Zhou et al. 2023). Although the recovery and repeatability of Sr are high and reliable, however, it is laborious, time consuming since one precipitation is not enough to separate  $^{90}\text{Sr}$  from interferences and poses great health risks to the operator because of the use of the offensive fuming nitric acid (Shao et al. 2018). The procedures involved in this technique include the separation of Sr from usually large chunk of Ca (usually repeated 3 to 5 times), separation of Sr from Ba, and then lastly the separation and purification of Sr from Y (Vajda and Kim 2010).

### **2.5.2. Liquid-liquid extraction (LLE)**

This separation technique is based on the different solubilities of a solute in two partially miscible liquid solvents. It involves using organic extractants to remove radionuclides from acid solution. The strontium is extracted from aqueous stage into an organic solvent containing hydrophobic ligand (also known as extractant) to form a stable electrically neutral complex with strontium. Examples of extractants that have been used to separate  $^{90}\text{Sr}$  and  $^{90}\text{Y}$  include di(2-

ethylhexyl) phosphoric acid (HDEHP), tributyl phosphate (TBP), Thiopheneyl trifluoroacetone (TTA) and trioctylphosphine oxide (TOPO) (Zhou et al. 2023). This technique is easy, quick, and efficient as the recovery and selectivity of strontium is high. However, the organic solvents used in this technique are usually toxic, volatile, and expensive (Shao et al. 2018).

### **2.5.3. Ion exchange chromatography**

This technique uses the different ions and polar molecules affinities unto ion exchangers to separate the target analyte from interfering elements. This technique is characterized by having high selectivity and can be used for simultaneous multi-radionuclide separation (Shao et al. 2018). Some commonly ion exchange resins employed for separating  $^{90}\text{Sr}$  or  $^{90}\text{Y}$  include Dowex-50, AG 1-X8, Zeokarb 225, Amberlite IR-120 and AG 50W-X8. These ion exchange resins are characterized with high molecular weight organic polymers having different functional groups covalently bound to the network of polymers (Vajda and Kim 2010). Though this technique can handle large volumes of samples and can be applied to different matrices, however, it takes a long time, less effective, has small exchange capacity, and has tedious analytical process because of complicated procedures (Zhou et al. 2023).

### **2.5.4. Adsorption**

This is a technique that involves a process of transferring target analytes from the aqueous phase to an absorbent's surface. This technique is considered as one of the most effective methods of removing environmental pollutants. It is cost-effective, has high capacity and flexibility in operation, and generates little waste. Examples of organic and inorganic adsorbents that have been developed to remove strontium through aquatic media include natural zeolites, ammonium molybdophosphate composites, hydroxyapatites, porous carbon composites, graphene oxides, metal sulfides, metal-organic frameworks (Kim et al. 2022). Though adsorption is economically

feasible and efficient, increasing the selectivity of adsorbents to target remains a significant challenge (Zhou et al. 2023).

### **2.5.5. Electrosorption**

This technique combines adsorption and electrochemistry through non-Faradic process independent of electron gain or loss to remove heavy metals from aqueous solutions. Examples of electrosorption techniques that have been developed include half-wave rectified alternating current electrochemical method and asymmetrical alternating or direct current electrochemical method. Although this technique is a rapidly developing method for the removal of strontium from industrial wastes, it's highly efficient, and generates no waste (Zhou et al. 2023).

### **2.5.6. Extraction chromatography (EC)**

Extraction chromatography is also known as solid phase extraction (SPE) chromatography. Extraction chromatography combines multistage features of column chromatography which requires low-cost input, simple operation, and easier material with high selectivity of solvent extraction (Cao et al. 2022). EC uses the basic principle of liquid-liquid extraction (a method of separating materials depending on how differently a solute dissolves in two liquid solvents that are somewhat miscible), but the liquid extractants are absorbed on the surface of an inert solid support material (Zhou et al. 2022). Advantages of EC include it involves less hazardous waste is produced, fast exchange kinetics due to the extraction process taking place in the thin surface layer allowing good contact of the reagents, and more effective separation due to the chromatographic technique (Vajda and Kim 2010).

The determination of pure beta emitter procedure which involves chemical separation of strontium from other elements by appropriate methods can be somewhat difficult because there are several steps involved in the isolation of small amounts of strontium from complex matrices.

There are also challenges when separating strontium from calcium because of their similarities in chemical behavior (Grahek et al. 2018). The oldest and most popular method for separating strontium is the selective precipitation procedure, which is based on the difference in solubilities of Ca and Sr nitrates in fuming nitric acid. However, due to the aggressiveness and corrosive hazard of fuming nitric acid, it has been increasingly replaced by solid phase extraction on specific resins such as Sr resin (Grahek et al. 2018; Vajda and Kim 2010).

#### ***2.5.6.1. Strontium extraction chromatography resin***

Extraction chromatography resin consists of collections of beads packed into a column to selectively absorb a particular chemical. These beads contain three main components: the inert support matrix, the stationary phase, and the mobile phase. (Horwitz et al. 1992). The inert support matrix phase typically consists of an organic polymer or porous silica ranging in size from 50 to 150  $\mu\text{m}$  in diameter. It provides a structural support system for the stationary phase much like a sponge (Horwitz et al. 1992). The stationary phase consists of a liquid extractant consisting of a single compound or a mixture, while the mobile phase is usually an acid solution, e.g., nitric, or hydrochloric acid. Sometimes, oxalic or hydrofluoric acids are used for stripping of strongly retained metal ions from columns, or to enhance selectivity (Horwitz et al. 2015).

For the radiochemical separation of radionuclides from interfering elements present in complex matrices, novel specific resins (extractants) such as Sr resin (Sr\*Spec) and AnaLig\*Sr01 (or SuperLig\*620) resin have been developed in the last few years (Marchesani et al. 2022). AnaLig\*Sr01 resin was developed by covalently bonding of a ligand, most likely a variation of an 18-crown-6 (18C6) structure, onto silica gel (Grahek et al. 2018). The Sr resin by Eichrom is prepared by sorbing of crown ether, 4,4'(5')-di-t-butylcyclohexano 18-crown-6 dissolved in 1-octanol as its extractant (Figure 2.1). The extraction equilibrium is described by Equation 2.3. It is

reported to be an effective method used for the separation of Sr from nitric acid media (Grahek et al. 2018; Vajda and Kim 2010). Figure 3.5 shows a ring of oxygen which acts for bonding in the center of this molecule.



The Sr resin acts primarily to separate strontium from other ions because of the space inside the ring of oxygen molecules. The strontium ion can fit right inside this ring of oxygen atoms due to an effective ionic radius of 118 picometers (pm). This resin is effective in separating strontium from other ions by exploiting the varying acid dependencies of different ions under different acid concentrations. Figure 2.2 shows the acid dependency of binding affinity (k') for different ions at 23 to 25°C for Sr resin. A trend may be observed in this graphical representation. The ability to absorb strontium (Sr (II)) by the column increases to a maximum at 8 M HNO<sub>3</sub>, while the concentrations of all other ions sharply fall. The ability to elute only strontium once absorbed onto the column is another reason why these columns work effectively in strontium separation. An acid concentration of 0.01M HNO<sub>3</sub> is sufficient to selectively to elute the strontium (Eichrom 2023).

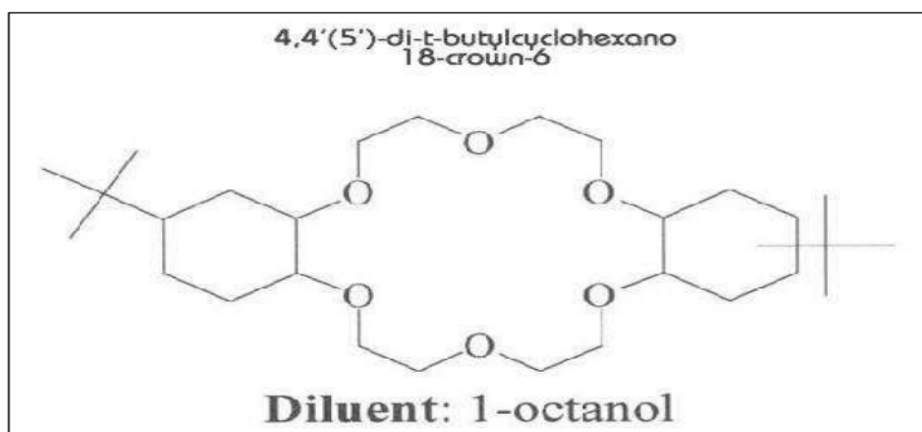


Figure 2.1. Eichrom's Sr resin extractant (Source: Eichrom 2023)

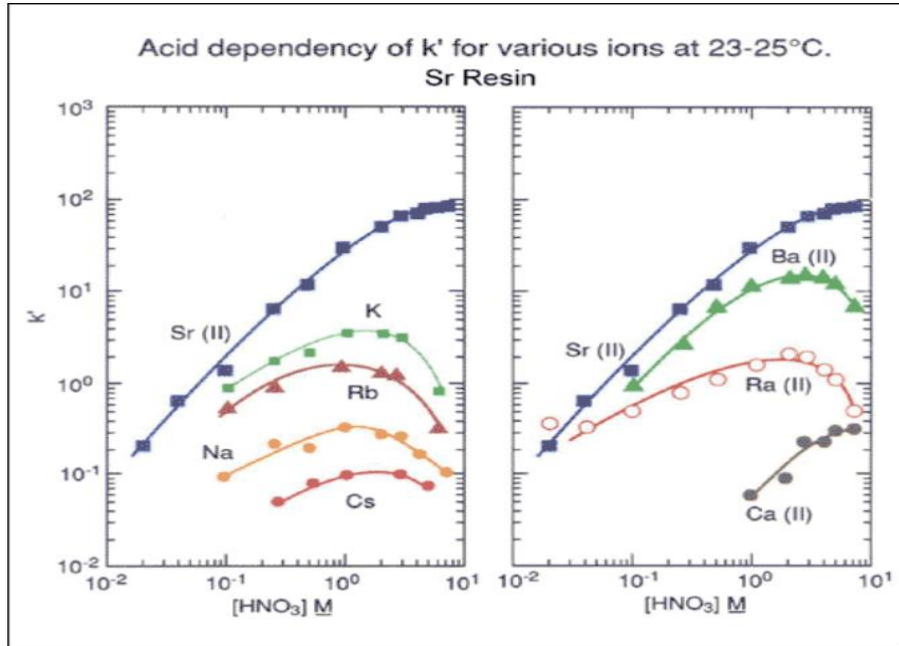


Figure 2.2. Acid dependency of  $k'$  for different ions at 23 to 25°C Sr resin (Eichrom 2023)

## 2.6. Measurement of $^{90}\text{Sr}$ in environmental samples

The techniques used for detecting  $^{90}\text{Sr}$  include gas ionization detectors (Geiger Muller and proportional counters), liquid scintillation counter(s) (LSC), semiconductor detectors and Cerenkov counters. The measurement of  $^{90}\text{Sr}$  can be accomplished using either directly measuring the separated or isolated  $^{90}\text{Sr}$  or by an indirect measurement through its daughter nuclide,  $^{90}\text{Y}$  (Lopes et al. 2014).

Direct measurement of  $^{90}\text{Sr}$  involves measuring  $^{90}\text{Sr}$  immediately after separation, ignoring the sample matrix and the ingrowth of  $^{90}\text{Y}$ . This method is appropriate for samples that need to be measured rapidly to assess  $^{90}\text{Sr}$  contamination such as in a nuclear accident. The second method examines the total beta spectrum of  $^{90}\text{Sr}$  and  $^{90}\text{Y}$  after they reach secular equilibrium. It takes about two weeks for secular equilibrium for secular equilibrium to be reached. The third method involves analyzing the activity of  $^{90}\text{Y}$  from  $^{90}\text{Sr}$ . In this case, the separation of  $^{90}\text{Y}$  from  $^{90}\text{Sr}$  after the

ingrowth is required but the total ingrowth of  $^{90}\text{Y}$  is not required. The last technique involves analyzing the activity of  $^{90}\text{Y}$  by Cerenkov counting after ingrowth of  $^{90}\text{Y}$ . It is unnecessary to segregate  $^{90}\text{Sr}$  from  $^{90}\text{Y}$  in this type of sample due to the low Cerenkov  $^{90}\text{Sr}$  counting efficiency of about 1.4% in contrast to the higher counting efficiency of 57% for  $^{90}\text{Y}$  (Shao et al. 2018)

### **2.6.1. Liquid scintillation counting (LSC)**

Liquid scintillation counting is a conventional radiometric technique for measuring beta emitting radionuclides and those that decay by electron capture. The main benefits of LSC include high counting efficiency, relatively simple and fast measurement which is suitable for the rapid analysis of  $^{90}\text{Sr}$ . LSC is commonly used in routine monitoring work in nuclear facilities and medical research. It is a key technique used for naturally occurring radionuclides such as  $^{226}\text{Ra}$ ,  $^{228}\text{Ra}$  and  $^{222}\text{Rn}$  (Hou, 2018). It is also a major technology used in monitoring the environment for radionuclide releases such as  $^{14}\text{C}$ ,  $^3\text{H}$ ,  $^{99}\text{Tc}$ ,  $^{36}\text{Cl}$ ,  $^{55}\text{Fe}$ ,  $^{89,90}\text{Sr}$ , and  $^{241}\text{Pu}$  associated with nuclear fuel cycle activities which include fuel enrichment, fuel fabrication, power generation and fuel reprocessing (Hou and Dai 2020).

### **2.6.2. Cerenkov counting**

Cerenkov radiation is described as a blue light that is produced when an electrically charged particle travels faster than the phase velocity of light in a transparent medium (Zhou et al. 2022). Cerenkov radiation is made up of a continuous spectrum of wavelengths extending from the ultraviolet region into the visible part of the spectrum up to about 420 nm (L'Annunziata 2004). The Cerenkov counting method employs fast electrons from beta decay moving in a dielectric and transparent medium that cause local electronic polarization of molecules, which rapidly return to the ground state releasing electromagnetic radiation called Cerenkov radiation (Tayeb et al. 2014).

The Cerenkov counting method uses a transparent solution such as water or alcohol to replace the organic cocktail scintillator (Wang 2013). The minimum beta energy for a radionuclide to cause Cerenkov light production in water is 263 keV. However, to obtain a reasonable efficiency. It is desirable for the beta radiation energy to exceed 1 MeV to induce Cerenkov radiation (Hou and Dai 2020; Al-Masri 1996). Beta emission energy of  $^{90}\text{Sr}$  ( $E_{\text{max}} = 0.546 \text{ MeV}$ ) is not suitable for direct measurement by Cerenkov counting because its energy is relatively low and hence not easily detectable. The Cerenkov counting technique is highly selective for  $^{90}\text{Y}$  ( $E_{\text{max}} = 2.28 \text{ MeV}$ ) and  $^{89}\text{Sr}$  ( $E_{\text{max}} = 1.46 \text{ MeV}$ ) where high Cerenkov counting efficiencies (>40%) can be anticipated.

Advantages of Cerenkov counting include simple sample preparation, satisfactory counting efficiency, low background, no addition of chemical quenching and no chemiluminescence (Zhou et al. 2022; Al-Masri 1996). Color quenching effects are a common problem in Cerenkov counting techniques and could strongly affect Cerenkov counting. To overcome this problem, a correction by the sample channel ratio (SCR) method or quench correction curve method can be applied. However, the SCR method is time-consuming to select the optimal counting window and has a limited application for low activity radionuclide counting while the quench curve method can only be carried out using a liquid scintillation analyzer equipped with a high energy gamma source having photon energy greater or equal to 430 keV (e.g.,  $^{152}\text{Eu}$ ). Quench curve correction using an external gamma source requires high yield due to the lower intensity of Cerenkov light (Yang et al. 2021; Tayeb et al. 2014). Therefore, to find a more effective solution to the Cerenkov counting technique problem, triple-to-double coincidence ratio (TDCR) techniques have been developed.

### 2.6.3. Triple-to-double coincidence ratio (TDCR)

The TDCR technique is an absolute standardization method of LSC for the determination of the activity of pure beta emitting and pure electron capture (EC) nuclides. The TDCR technique uses a triple coincidence counting method unlike the conventional double coincidence counting techniques. The TDCR technique requires a liquid scintillation analyzer (LSA) equipped with three photomultiplier tubes (PMTs) and two different coincident outputs as shown in Figure 2.3 (L'Annunziata 2004). Application of the TDCR technique requires the integration of a theoretical calculation describing counting efficiency. This function is based on physical and statistical model of the distribution of scintillation photons and their detection probability in the LSC (Hou and Dai 2020). The application of the TDCR is used for the rapid evaluation of interference (e.g., color quenching and sample geometry) on the activity measurements since triple-to-double coincidence count ratios significantly decrease in the presence of interference (Tayeb et al. 2014).

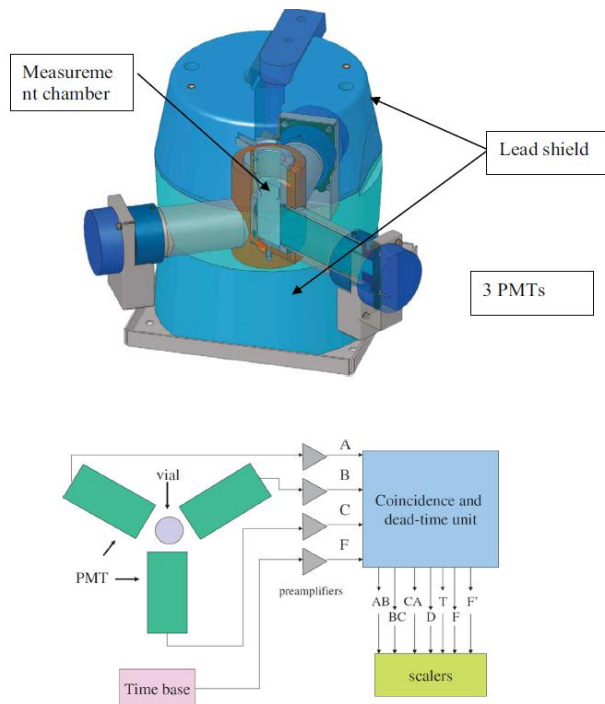


Figure 2.3. Diagram of the principle of TDCR system in the Hidex 300 SL (Source: Hou 2018).

### ***2.6.3.1. TDCR liquid scintillation counting***

Triple and double coincidences are both measured in TDCR based LSC to obtain TDCR values for efficiency calculations. Since triple coincidences are more sensitive to chemical and color quenching than double coincidences, a correlation between the quench level or counting efficiency and measured TDCR value can be established for quench correction. TDCR is a universal method applicable for both chemical and color quenching for aqueous and organic samples, and for different cocktails for a range of radionuclides unlike the external standard methods. Therefore, an external standard for monitoring quench level is not needed when using the TDCR liquid scintillation counting. The TDCR efficiency calculation method is suitable for routine analysis of beta-emitting nuclides in samples with different quench levels because the TDCR values usually approximate the overall counting efficiencies (Hou 2018; Yang et al. 2021; Hou and Dai 2020).

### ***2.6.3.2. TDCR Cerenkov counting***

The TDCR technique can be employed to correct quenching effects on Cerenkov efficiency. The TDCR parameter values decrease with increasing quench level since triple coincidence counts are more sensitive to quench compared to the double coincidence counts. The TDCR Cerenkov counting technique has been employed for direct and rapid determination of high-energy pure beta emitting radionuclides such as  $^{90}\text{Sr}/^{90}\text{Y}$ ,  $^{32}\text{P}$ ,  $^{204}\text{Tl}$ , and  $^{106}\text{Rh}$  in environmental samples (Yang et al. 2021). Tayeb et al. (2014) for example, evaluated interferences on measurements of  $^{90}\text{Sr}/^{90}\text{Y}$  using the TDCR Cerenkov counting technique. Interferences of sample geometry such as sample vial type, volume composition and sample color on Cerenkov counting efficiency of  $^{90}\text{Y}$  could be corrected by the TDCR Cerenkov counting.

## Chapter 3 : Methodology

### 3.1. Chemicals and materials

All chemicals used are American Chemical Society (ACS) reagent grade. Some of the chemicals used include nitric acid ( $\omega=70\%$ ) from Fisher Chemical<sup>1</sup>, hydrogen peroxide (30% concentration) from MACRON<sup>2</sup>, Sr carrier solution from Thermo Fisher Scientific<sup>3</sup>, Oxalic acid dihydrate ( $C_2H_2O_4 \cdot 2H_2O$ ) from Merck<sup>®4</sup>, Ultima Gold<sup>™</sup> uLLT LSC cocktail from Perkin Elmer Inc.<sup>5</sup>, <sup>85</sup>Sr from Eckert and Ziegler<sup>6</sup>, and <sup>90</sup>Sr+<sup>90</sup>Y from Eckert and Ziegler. A muffle furnace from Barnstead Thermolyne<sup>7</sup> was used for drying the soil samples while vacuum box was used for <sup>90</sup>Sr collection.

### 3.2. Instrumentation and software

High purity germanium (HPGe) gamma radiation detectors are available at the Environmental monitoring Laboratory (EML) (Canberra GC2520<sup>8</sup>) was used to determine the activity of <sup>137</sup>Cs while ORTEC GEM-FX8530P4<sup>9</sup> was used to determine the chemical recovery of <sup>85</sup>Sr as it emits discrete gamma-photons at 514 keV (Appendix A: Certificates). The <sup>85</sup>Sr standard efficiency was determined to be 0.0226 (Appendix B). The extraction chromatographic separation of <sup>90</sup>Sr was carried out using Sr-Resin<sup>®</sup> cartridges manufactured by Eichrom<sup>10</sup>. Hidex 300 SL<sup>11</sup>

---

<sup>1</sup> Fisher Chemical, USA

<sup>2</sup> MACRON FINE CHEMICALS by Avantor Performance Materials, LLC; Radnor, PA, USA

<sup>3</sup> Thermo Fisher Scientific, USA

<sup>4</sup> Merck, Sigma-Aldrich, Inc. St. Louis, MO, USA

<sup>5</sup> Perkin Elmer Inc. Shelton, CT, USA

<sup>6</sup> Eckert and Ziegler Isotope Products (Valencia, CA, USA)

<sup>7</sup> Barnstead Thermolyne by Thermo Scientific, MA, USA

<sup>8</sup> Canberra, Connecticut, USA

<sup>9</sup> Ortec, Oak Ridge, TN, USA.

<sup>10</sup> Eichrom Technologies Inc. IL, USA

<sup>11</sup> Hidex Oy, Turku, Finland.

LSC (Figure 3.1) was used with Ultima Gold™ uLLT scintillation cocktail for  $^{90}\text{Sr}$  determination. MikroWin 300 SL version 5.60 software was employed for LS counting on the Hidex.

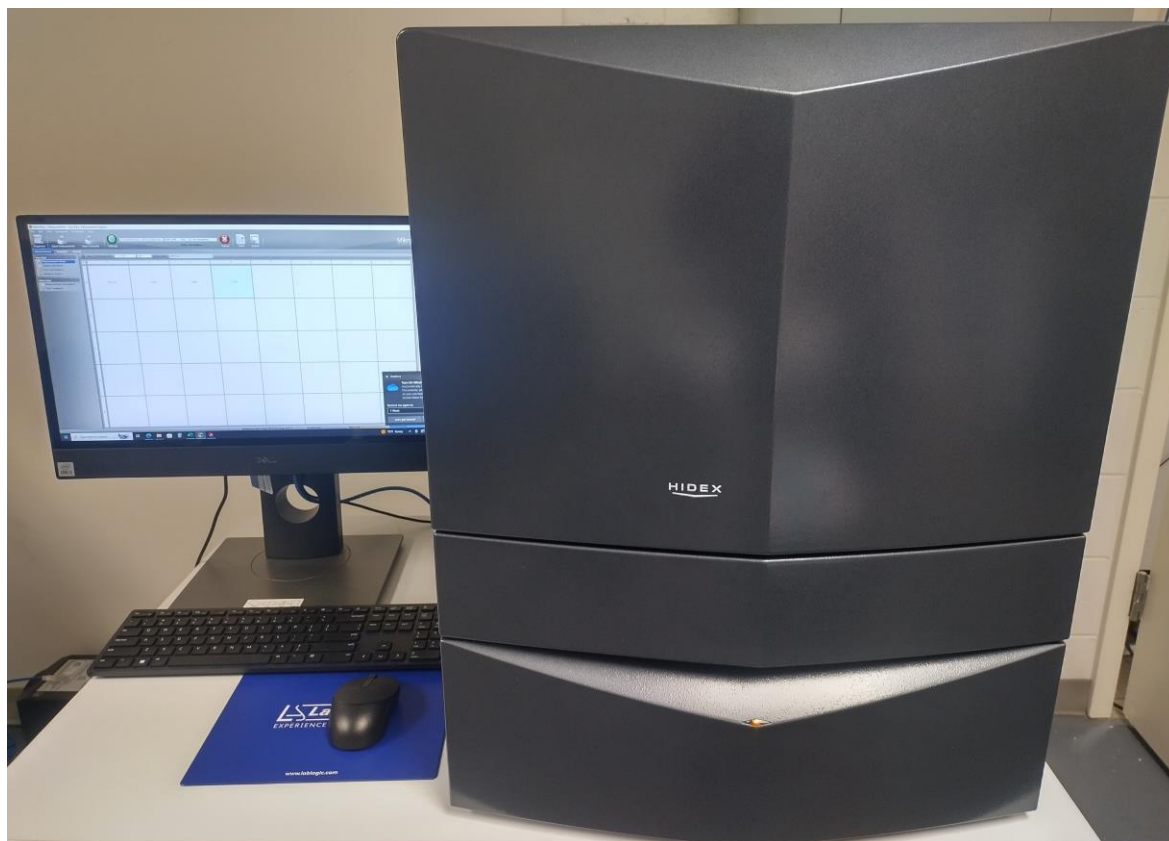


Figure 3.1. Hidex 300 SL liquid scintillation counter equipped with TDCR technology.

### 3.3. Sample procedures

The overall procedures that were used for this study are divided into separate steps and observations, which include 1) sample collection 2) sample preparation 3) strontium separation and 4) Strontium measurement. Figure 3.7 shows the flowchart of analysis procedure of samples and strontium separation and purification.

### **3.4. Sample collection**

The mass of soil and vegetation samples needed to achieve a minimum detectable concentration of  $^{137}\text{Cs}$  and  $^{90}\text{Sr}$  depends on several factors, including the background radiation, the efficiency of the detecting system, and the desired level of confidence in the measurement result. A sample size of several tens of grams to a few hundred grams is usually sufficient for most environmental monitoring programs (USNRC 2020).

#### **3.4.1. Data quality objective**

The Data Quality Objective (DQO) helps managers to decide what kind, caliber, and quality and quantity of data that will be sufficient for making environmental decisions. Before any data is collected, the DQO enables decision-makers to specify the limits on the likelihood of making allowable degrees of decision error (VanHorn and Harney 2007). According to the guidance for the data quality objectives process used for environmental monitoring program by INL (2017), the DQO process involves seven steps with each having specific outputs.

The first step in DQO was to state the problem. The problem statement is to assess the long-term deposition of radionuclides resulting from activities at the INL in the soils surrounding the INL Site and to characterize the radionuclide inventory in the soils within the INL boundaries and in the surrounding areas.

The second step was to identify the goals of the study. This involves identifying the decisions and the potential actions that will be influenced by the data collected. This was achieved by defining the principal study questions (PSQs) and the alternative actions that may result from addressing those questions into decision statements (DSs). The monitoring effort is designed to address two PSQs:

PSQ1: What is the baseline inventory of interested radionuclides in soils in the areas under investigation? DS1: Concentration of radionuclides of interest in the soil should be determined and monitoring data should be utilized to update the baseline inventory over time.

PSQ2: What is the long-term deposition of radionuclides in soils resulting from INL activities? DS2: Air models should be employed to determine the most probable locations of radionuclide deposition due to INL activities and these soils should be monitored for long-term deposition resulting from Site activities.

The third step was to identify information inputs. This includes identifying radionuclides of interest in the soils in areas surrounding INL; quantifying the concentration of the radionuclide in the soils in the understudied region; historical radionuclide concentrations in the soils for the studied areas; wind patterns within the region to locate the places most likely to be exposed to radioactive fallout due to INL activities; identifying areas that may have increased inventories due to past activities; identifying possible source terms of radionuclides; and locating population centers in the vicinities around the Site.

The fourth step was to define the boundaries of study. This includes physical boundaries (areas based on proximity to source terms and the public), temporal boundaries (time intervals between soil sample collections at a location, which may have been as early as the 1970s, up until soil monitoring is no longer measured under the program); and physical considerations (these are constraints in collection of data such as lack of undisturbed soil, access to properties for sample collection, cost of sampling and analysis, and time needed to collect and analyze the samples).

The fifth step was to develop an analytical approach. This step outlines the analytical strategy, which necessitates defining the action levels, suitable estimators, and the population parameters that will be utilized to make decisions.

The sixth step was to specify performance or acceptance criteria. This step defines the decision rules and estimation uncertainty. The background doses were selected at a 95% confidence level, and the other uncertainties were reduced by making sure that adequate data were gathered at each location and that the best sampling practices were followed.

The seventh step was to develop a detailed plan for obtaining data. The statistical methods require that the sampling locations are established using the most basic probability sampling design method called random sampling. For this study, a composite sampling technique was employed. This involves collecting five individual samples at the corner of a 10×10-meter square and a sample at the middle of the 10×10-meter square sample area. This was done to minimize the heterogeneity at each sampling location. All the samples were mixed, and a single composite sample was sent to the lab for analysis.

Figure 3.2 represents the flowchart of the  $^{90}\text{Sr}$  separation employed for this study.

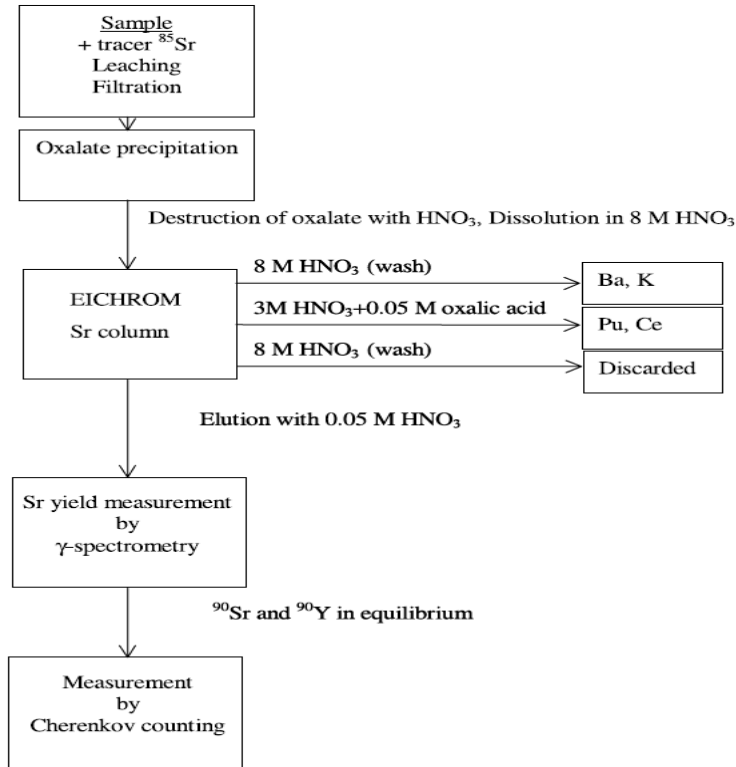


Figure 3.2. Flowchart of  $^{90}\text{Sr}$  separation (Source: Solatie et al. 2002)

### 3.5. Sample preparation

Soil samples were collected between 07/26/22 to 08/04/22 from locations around the Idaho National Laboratory. After the samples were collected, they were taken to the laboratory and dried in an oven for 24 hours at 110°C, homogenized and sieved using <2 mm sieve for gamma spectroscopy measurement to determine the activity concentration of  $^{137}\text{Cs}$ . 10 g of dried and homogenized soil sample from each location was ashed in a muffle furnace at 500 °C for 15 hours before subjecting them to strontium extraction process.

### 3.6. Strontium separation

The separation of strontium from the samples involves processes such as leaching, filtering, pre-loading, loading, rinsing and elution. The leaching process entails placing the digested samples into a reflux boiler and adding 1 ml of Sr carrier ( $\text{Sr}^{2+}$  carrier as strontium nitrate, 20 mg/ml in

each). 4 mL of 8 M nitric acid ( $\text{HNO}_3$ ), 1-mL hydrogen peroxide ( $\text{H}_2\text{O}_2$ ) and 2-mL 16 M  $\text{HNO}_3$  was added. The solution was kept at 8 M  $\text{HNO}_3$  and boiled for 60 minutes. At the 30-minute mark, additional items (4 mL of 8 M  $\text{HNO}_3$ , 1-mL of  $\text{H}_2\text{O}_2$  and 1-mL of 16 M  $\text{HNO}_3$ ) were added to the reflux boiler to keep the sample from drying out. Additionally, 1-ml of 16 M  $\text{HNO}_3$  and 1-ml  $\text{H}_2\text{O}_2$  was used to keep the overall concentration of the mixture's nitric acid concentration at 8 M and making sure the pH is kept at 1 with the use of a pH meter.

After the completion of boiling for an hour, the sample mixture was filtered by passing it through a Buchner funnel into a vacuum flask to separate the aqueous phase from the soil. 6-ml of 8 M  $\text{HNO}_3$  was applied to wash the boiling flask in 1-ml increments, this rinse was conducted five times to wash the soil media and ensure the maximum transfer of strontium to the aqueous phase.

Figure 3.3 shows the extraction chromatography setup. The pre-loading step involved setting up the extraction chromatography vacuum box to provide a 5-inch Hg vacuum pressure differential. This allows for quicker operation of the column at a flow rate of 3 ml/min attached with a 10 ml syringe. The column was packed with Sr extraction chromatography resin-B (produced by Eichrom® Technologies, Inc.) with each resin having small particle size of 50 to 100  $\mu\text{m}$ . The Sr resin was first preconditioned by rinsing with 5 ml of 8 M  $\text{HNO}_3$ .

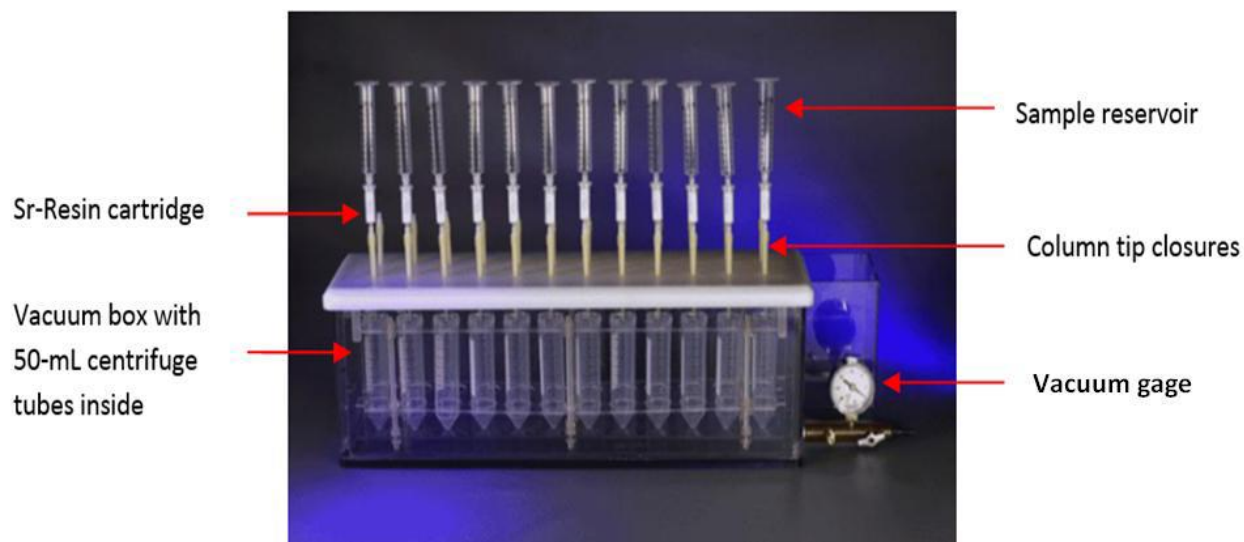


Figure 3.3. Extraction chromatography setup (Tayeb 2015)

After the preconditioning, the next step was loading the Eichrom column with the filtered aqueous strontium solution from the vacuum flask. After emptying, the vacuum flask was rinsed with 5-ml of 8 M  $\text{HNO}_3$  to ensure all the strontium was transferred out of the flask into the column. To effectively absorb the  $^{90}\text{Sr}$  into the column, 5 ml of 8-M  $\text{HNO}_3$  was added to the column. Each sample was divided into two different aliquots. The first aliquot was spiked with 43 to 49 Bq (decayed to the day of counting) of stable  $^{85}\text{Sr}$  to determine the radiochemical yield while the second aliquot was unspiked to determine  $^{90}\text{Sr}$  activity.

The rinsing step involves adding 5 ml of 3-M  $\text{HNO}_3$  + 0.05-M oxalic acid to the column to wash off impurities and prevent the retention of actinide elements. The column is a competitive complexing agent (Ball 2015). After rinsing with 5 ml of 3-M  $\text{HNO}_3$  + 0.05-M oxalic acid, 5 ml of 8-M  $\text{HNO}_3$  was added to the column. All the rinsed liquid was disposed of as waste. The time required for liquid to drain to waste collection beaker was recorded as the Sr-90/Y-90 separation time.

The last stage in the strontium separation process is the elution. This step served to remove strontium from the column. The strontium was stripped using 15 ml of 0.05-M HNO<sub>3</sub> that was passed through the column. Details of how different reagents were prepared can be found in Appendix C.

### 3.7. Validation of analytical method

To benchmark the effectiveness of the analytical method (separation process), a mixed analyte performance evaluation program (MAPEP) soil reference sample was used. The MAPEP soil (MAPEP-22-MaS-47 and MAPEP-23-MaS-48) samples with known <sup>90</sup>Sr activity was used to determine the performance of the methodology. One of the soils was spiked with 80 Bq of <sup>85</sup>Sr and subjected to the separation process, and then analyzed on the HPGe gamma detector to determine the chemical recovery. The chemical recovery (R) of <sup>85</sup>Sr was determined using Equation 3.2. A duplicate of one of the MAPEP soils was also subjected to the separation process and counted on the LSC to determine the reproducibility of the result.

$$R = \frac{A_2}{A_1} \times 100 \quad (3.2)$$

where  $A_1$  is the activity of <sup>85</sup>Sr added to the soil sample before the chemical separation and  $A_2$  is the activity of <sup>85</sup>Sr in the sample after the chemical separation. The activity of <sup>85</sup>Sr in the sample after the chemical separation,  $A_2$  was determined using Equation 3.2.1.

$$A_2 = \frac{C_R}{\eta} \quad (3.2.1)$$

where  $C_R$  is the count rate of sample counted on the gamma detector after chemical separation in count per seconds while  $\eta$  is the <sup>85</sup>Sr standard efficiency determined on the gamma detector.

The counting efficiency that confirms the accuracy of the radioactivity measured by the LSC was determined using  $^{90}\text{Sr}+^{90}\text{Y}$  standard solution. The count rate represented by count per seconds (cps) of the standard samples counted for 3600 seconds was determined using the current activity of the standard. The counting efficiency was determined using Equation 3.3. Details of how the calculation was obtained can be seen in Appendix D.

$$\varepsilon = \frac{R_{std} - R_b}{A_{std}} \quad (3.3)$$

where  $R_{std}$  is the net count rate of  $^{90}\text{Sr}+^{90}\text{Y}$  standard solution;  $R_b$  is the background count rate and  $A_{std}$  is the decay corrected activity of the  $^{90}\text{Sr}+^{90}\text{Y}$  standard solution.

### 3.8. Strontium measurement

Strontium-90 was measured using direct LSC counting immediately after  $^{90}\text{Sr}$  separation and recounting two weeks after  $^{90}\text{Y}$  ingrowth. The direct LSC measurement made immediately after  $^{90}\text{Sr}$  separation, was conducted using the Hidex 300 SL LSC. Samples were darkened for 2 hours to eliminate the influence of scintillation cocktail fluorescence (Asgharizadeh et al. 2009). All samples were counted for 60 minutes (3600 seconds).

### 3.9. Activity concentration calculation

The activity concentration of  $^{137}\text{Cs}$  (Bq/kg) was calculated using Equation 3.4.

$$A_{Cs-137} = \frac{N_{net}}{\varepsilon \times \gamma \times M \times t} \quad (3.4)$$

where  $A_{Cs-137}$  is the activity of  $^{137}\text{Cs}$  in the sample (Bq/kg);  $N_{net}$  is the net peak area count;  $\varepsilon$  is the absolute full energy peak efficiency of HPGe detector;  $\gamma$  is the gamma yield;  $M$  represents mass of the sample (kg); while  $t$  is the time of sample count.

To test the veracity of the results, the activity concentration was determined using the traditional methods (ASTM) and the TDCR method.

The activity of  $^{90}\text{Sr}$  in the samples immediately after separation was calculated using Equation 3.5 (ASTM 2009).

$$A_{\text{Sr-90}} = \frac{R_n}{\varepsilon \times R \times m \times \left[ 1 + \left( \frac{\lambda_Y}{\lambda_Y - \lambda_{\text{Sr}}} \right) \left( e^{-\lambda_{\text{Sr}} \times \frac{(T_1 + T_2)}{2}} \right) - \left( e^{-\lambda_Y \times \frac{(T_1 + T_2)}{2}} \right) \right]} \quad (3.5)$$

where  $A_{\text{Sr-90}}$  is the activity of  $^{90}\text{Sr}$  in the sample (Bq/kg);  $R_n$  is the net count rate of sample;  $\varepsilon$  is the counting efficiency of  $^{90}\text{Sr}$  standard;  $R$  is the chemical recovery;  $m$  is the mass of the sample;  $\lambda_Y$  is the decay factor of  $^{90}\text{Y}$ ;  $\lambda_{\text{Sr}}$  is the decay factor of  $^{90}\text{Sr}$ ;  $T_1$  is the elapsed time between chemical separation and the beginning of the count time; and  $T_2$  is the elapsed time between chemical separation and the end of the count time.

The activity of  $^{90}\text{Sr}$  in the samples immediately after separation using the TDCR method was calculated using Equation 3.7 (Dai et al. 2013).

$$A_{\text{Sr-90}} = \frac{\frac{CR_s}{(\varepsilon_s)} - \frac{CR_b}{(\varepsilon_b)}}{R \times w \times (D_{\text{Sr}} + I_Y)} \quad (3.6)$$

where  $A_{\text{Sr-90}}$  is the activity of  $^{90}\text{Sr}$  in the sample (Bq/kg);  $CR_s$  represents count rate of sample;  $CR_b$  is the count rate of blank;  $\varepsilon_s$  and  $\varepsilon_b$  are the sample and blank counting efficiencies respectively;  $R$  is the chemical recovery;  $w$  is the weight fraction of sample measured of the eluate transferred;  $D_{\text{Sr}}$  is the decay factor of  $^{90}\text{Sr}$ ; and  $I_Y$  is the ingrowth factor of  $^{90}\text{Y}$  from  $^{90}\text{Sr}$ . The decay factor of  $^{90}\text{Sr}$ ,  $D_{\text{Sr}}$  and the ingrowth factor of  $^{90}\text{Y}$  from  $^{90}\text{Sr}$  was calculated using Equation 3.6.1 and 3.6.2 respectively.

$$D_{\text{Sr}} = e^{-(T_1 - T_0)\lambda_{\text{Sr}}} \quad (3.6.1)$$

where  $T_1$  is the time of start of LSC of  $^{90}\text{Sr}$  on Hidex,  $T_0$  is the time of the end of  $^{90}\text{Sr}$  extraction on the Sr-Resin and  $\lambda_{\text{Sr}}$  is the  $^{90}\text{Sr}$  decay constant (in  $\text{sec}^{-1}$ ).

$$I_Y = \frac{\lambda_Y}{\lambda_Y - \lambda_{\text{Sr}}} \times (e^{-(T_1 - T_0)\lambda_{\text{Sr}}} - e^{-(T_1 - T_0)\lambda_Y}) \quad (3.6.2)$$

where  $\lambda_Y$  is the  $^{90}\text{Y}$  decay constant (in  $\text{sec}^{-1}$ ).

The activity concentration of the soils was back calculated to the time of collection using Equation 3.7.

$$A_0 = \frac{A}{e^{-\lambda t}} \quad (3.7)$$

where  $A$  is the current activity;  $A_0$  is the initial activity;  $\lambda$  is the decay constant of  $^{90}\text{Sr}$ , and  $t$  is the time difference from initial to current activity).

### 3.10. Detection limit and minimum detectable activity

The detection limit ( $L_d$ ) is an a-priori estimate of the minimum value of the true net signal that can be accurately determined by a given detection system or measurement procedure (Kirkpatrick et al. 2013). It is defined as the number of net counts above the background which the detector will reliably detect a source with a 95% probability (Falkner 2018). The detection limit is determined by the quantity of counts and is not always equivalent to measured activity in the field (USNRC 2020). It is given by Equation 3.10.

$$L_D = 2.71 + 4.65\sqrt{C_b} \quad (3.10)$$

where  $C_b$  is the background counts.

The minimum detectable activity (MDA) is defined as the smallest amount of activity that can be detected by a detecting system above the background in specific measurement conditions

(Done and Loan 2016). It can also be defined as the activity value corresponding to the detection limit with a calibration factor applied to the detection limit. The MDA is given by Equation 3.11 known as the Curie equation (Curie 1968).

$$MDA = \frac{2.7+4.65\sqrt{B}}{t \times R \times \epsilon \times m} \quad (3.11)$$

where  $B$  is the total number of counts of the background sample;  $t$  is the counting time;  $R$  is the chemical recovery;  $\epsilon$  is the counting efficiency; and  $m$  is the mass of the sample in kg.

### 3.11. Uncertainty measurement

The uncertainty of measurement is an expression that states that for a given measurement result, there are infinite values dispersed about the result that are consistent with all the observations/data and the knowledge of the physical world, and that with varying credibility degrees attributed to the measurand. Uncertainty in a measurement can be considerably increased by incomplete knowledge of influencing quantities and their effects (ISO 2008).

The uncertainty of the activity concentration of Cesium-137 is given by Equation 3.12.

$$\sigma_{Cs-137} = A_{Cs-137} \sqrt{\left(\frac{\sigma_{CR_{Cs-137}}}{CR_{Cs-137}}\right)^2 + \left(\frac{\sigma_M}{M}\right)^2 + \left(\frac{\sigma_\epsilon}{\epsilon}\right)^2 + \left(\frac{\sigma_R}{R}\right)^2} \quad (3.12)$$

where  $A_{Cs-137}$  is the activity concentration of  $^{137}\text{Cs}$ ;  $\sigma_{Cs-137}$  is the 1-sigma uncertainty of the net count rate of  $^{137}\text{Cs}$ ;  $\sigma_E$  is the 1-sigma uncertainty of the counting efficiency,  $\sigma_R$  is the 1-sigma uncertainty of the chemical recovery and  $\sigma_m$  is the 1-sigma uncertainty of the sample mass.

The uncertainty of the activity concentration of Strontium-90 is given by Equation 3.14 (ASTM 2009).

$$\sigma_{Sr-90} = A_{Sr-90} \sqrt{\left(\frac{\sigma_{R_n}}{R_n}\right)^2 + \left(\frac{\sigma_\epsilon}{\epsilon}\right)^2 + \left(\frac{\sigma_R}{R}\right)^2 + \left(\frac{\sigma_m}{m}\right)^2} \quad (3.14)$$

where  $\sigma_{R_n}$  is the 1-sigma uncertainty of the net count rate;  $\sigma_{\epsilon}$  is the 1-sigma uncertainty of the counting efficiency,  $\sigma_R$  is the 1-sigma uncertainty of the chemical recovery and  $\sigma_m$  is the 1-sigma uncertainty of the sample mass.

### 3.12. Method validation by certified reference materials

The extraction chromatography process used was validated by the analysis of MAPEP reference materials. The results were analyzed using different statistical evaluation such as bias, accuracy, precision and trueness based on ANSI N13.30 criteria. The bias in measurement is the difference between the measured value ( $A_m$ ) and the reference value ( $A_r$ ). The bias from the reference values was calculated using Equation 3.15. The acceptable criterion of bias was set between -0.25 to 0.50 (ANSI 1996).

$$Bias = \left( \frac{A_m}{A_r} - 1 \right) \quad (3.15)$$

The relative precision is the dispersion of the measured value relative to the mean value. The relative precision is given by Equation 3.16. The criterion for relative precision to be acceptable is  $2\% \leq RP \leq 15\%$ .

$$RP = \frac{\text{Reported uncertainty}}{\text{Reported Result}} \times 100 \quad (3.16)$$

The accuracy of a statistical value is the degree to which the values obtained from a measurement are close to the actual value. The criterion for accuracy to be acceptable is given by Equation 3.17.

$$|Bias| \leq \frac{A_m}{A_r} \times 2.58RP \quad (3.17)$$

To evaluate the reproducibility of the methods, Equation 3.18 was used.

$$|A_1 - A_2| < 3(\sigma_1^2 + \sigma_2^2)^{1/2} \quad (3.18)$$

where

$A_1$  = concentration of the first sample

$A_2$  = concentration of the duplicate sample

$\sigma_1$  = uncertainty of the first sample

$\sigma_2$  = uncertainty of the duplicate sample

## Chapter 4 : Results And Discussions

### 4.1. Activity concentration of $^{137}\text{Cs}$ in soil samples

The results of  $^{137}\text{Cs}$  activity concentration are presented in Table 4.1. The minimum mean activity concentration of  $^{137}\text{Cs}$  in the locations evaluated was determined to be at Mud Lake #1 with a value of  $10.92 \pm 1.63$  Bq/kg. The MDA for this analysis is 2.79 Bq/kg located at Mud Lake #1. A maximum value of  $18.08 \pm 2.12$  Bq/kg was observed at Reno Ranch. These analyses were completed over an extended period of one month after the collection dates, and the activity of all the samples were decay corrected to the collection dates. The minimum detectable activity (MDA) in the measured soils varies from 2.79 to 4.2 Bq/kg over the period of analysis. All the measured values are less than the recommended federal screening limit for surface soil of 236.8 Bq/kg (NCRP 129). Using the Federal screening limit as a threshold of impact, based on the measurements, there is no impact of INL operations on the off-site environment.

### 4.2. Activity concentration of $^{90}\text{Sr}$ in soil samples

Table 4.2 shows the result of activity concentration of  $^{90}\text{Sr}$  in all the analyzed soil samples. The results of the two analyses methods used (ASTM and TDCR) were also shown. The values observed for  $^{90}\text{Sr}$  activity concentration in the soil samples are between  $0.43 \pm 3.74$  to  $16.13 \pm 4.15$  Bq/kg and between  $0.49 \pm 3.59$  to  $21.15 \pm 3.99$  Bq/kg for the ASTM and TDCR methods respectively. The average activity concentration of  $^{90}\text{Sr}$  is  $7.80 \pm 4.85$  and  $9.64 \pm 6.51$  Bq/kg in ASTM and TDCR methods respectively. The duplicates of samples carried out on soils from Crystal ice cave, Frenchman's cabin and Reno ranch using the ASTM and TDCR methods are provided for comparison with the values of the initial soil samples from these locations.

Table 4.1. Results of  $^{137}\text{Cs}$  analysis in soil samples

<b>Location</b>	<b>Latitude</b>	<b>Longitude</b>	<b><math>A_{\text{Cs-137}}</math> (Bq/kg)</b>	<b>MDA (Bq/kg)</b>
Atomic City	43.4523	112.77401	10.27±1.59	3.64
Blackfoot	43.22639	112.6736	4.46±1.23	3.55
Butte City	43.592184	113.254838	12.33±1.76	3.52
Carey	43.333949	113.828192	17.58±2.06	3.75
Crystal Ice cave	42.955306	113.213417	12.50±1.79	4.01
Crystal Ice cave	42.955306	113.213417	10.02±1.87	4.20
Dup				
FAA Tower	43.55438	112.53764	15.05±1.99	4.07
Frenchmen's Cabin	43.427775	113.05628	6.39±1.31	3.34
Frenchmen's Cabin Dup	43.427775	113.05628	5.27±1.28	3.54
Howe	43.80005	112.87399	12.14±1.69	3.59
Mud Lake #1	43.85418	112.51081	1.82±0.88	2.79
Mud Lake #2	43.78175	112.48699	6.91±1.30	3.33
Reno Ranch	44.01001	112.717901	18.08±2.12	4.00
Reno Ranch Dup	44.01001	112.717901	16.99±2.00	3.81
St. Anthony	43.99926	111.67754	14.43±1.82	3.35
Monteview	44.01001	112.45549	10.42±1.45	3.15
<b>Average</b>			<b>10.92±1.63</b>	<b>3.55</b>

These duplicate data verify the reproducibility of the separation process. Also, the average MDA is 18.22 Bq/kg in both methods used. However, locations such as Atomic City, Carey, Mud Lake #1 and Mud Lake #2 show relatively small values compared to the MDA. Therefore,  $^{90}\text{Sr}$  activity concentration in these locations are reported as below the detection limit concentration.

Table 4.2. Results of  $^{90}\text{Sr}$  analysis in soil samples

Location	Latitude	Longitude	Sample Counts	ASTM	TDCR	ASTM	TDCR
				$A_{\text{Sr-90}}$ (Bq/kg)	$A_{\text{Sr-90}}$ (Bq/kg)	MDA (Bq/kg)	MDA (Bq/kg)
Atomic City	43.4523	112.77401	1920	1.31±3.83	1.46±3.59	18.40	18.40
Blackfoot	43.22639	112.6736	1857	4.03±3.78	4.32±3.55	17.95	17.95
Butte City	43.592184	113.254838	1856	10.56±3.95	12.33±3.79	18.35	18.35
Carey	43.333949	113.828192	1910	0.43±3.74	0.49±3.59	18.40	18.41
Crystal Ice cave	42.955306	113.213417	1916	5.91±3.83	6.85±3.63	18.13	18.13
Crystal Ice cave Dup	42.955306	113.213417	1956	9.23±3.83	11.45±3.72	18.13	18.13
FAA Tower	43.55438	112.53764	2044	11.74±3.99	21.15±3.99	18.42	18.42
Frenchmen's Cabin	43.427775	113.05628	1988	16.03±4.00	19.28±3.90	17.91	17.91
Frenchmen's Cabin Dup	43.427775	113.05628	2056	16.13±4.15	19.03±3.95	18.25	18.25
Howe	43.80005	112.87399	2249	8.19±3.85	9.97±3.73	18.35	18.35
Mud Lake #1	43.85418	112.51081	1844	2.86±3.73	3.30±3.53	17.95	17.95
Mud Lake #2	43.78175	112.48699	1837	2.23±3.68	2.51±3.52	17.95	17.95
Reno Ranch	44.01001	112.717901	1972	7.40±3.99	8.56±3.69	18.33	18.32
Reno Ranch Dup	44.01001	112.717901	1970	7.14±3.95	7.88±3.69	18.33	18.35
St. Anthony	43.99926	111.67754	1900	9.94±4.30	10.77±3.72	18.21	18.21
Monteview	44.01001	112.45549	2045	11.71±3.95	14.92±3.86	18.42	18.42
<b>Average</b>				<b>7.80±4.85</b>	<b>9.64±6.51</b>	<b>18.22</b>	<b>18.22</b>

### 4.3. Comparisons of ASTM and TDCR methods in <sup>90</sup>Sr activity determination

Table 4.3 shows the summary statistics of the methods used in the determination of <sup>90</sup>Sr activity concentration.

Table 4.3. Summary statistics of the ASTM and TDCR methods

Variable	Observations	Obs. with missing data	Obs. without missing data	Min.	Max.	Mean	Std. dev.
ASTM	16	0	16	0.430	16.130	7.803	4.848
TDCR	16	0	16	0.490	21.150	9.642	6.508

To determine the normality of these two methods, the Shapiro-Wilk test was conducted on the data. The Shapiro-Wilk test is a hypothesis test that evaluates the normal distribution of a random sample. The null hypothesis ( $H_0$ ) of the Shapiro-Wilk test states that the data follows a normal distribution while the alternate hypothesis ( $H_1$ ) is that the data does not follow a normal distribution. Table 4.4 shows the result of the Shapiro-Wilk test as conducted on these sets of data. From the Table, the computed p-value is greater than the significance level, alpha (=0.05) for the two methods. Therefore, the null hypothesis was not rejected, and there is no evidence of deviation from normality.

Table 4.4. Shapiro-Wilk test on the ASTM and TDCR methods

	ASTM	TDCR
Test statistic (W)	0.959	0.948
p-value (Two-tailed)	0.639	0.462
Alpha	0.05	0.05

To test if there is a statistically significant difference between these methods, a two-tailed test was carried out. Table 4.5 shows the t-test for the two independent samples otherwise known as two-tailed test. At the 95% confidence level for the comparisons, the percentage difference is statistically insignificant. The null hypothesis ( $H_0$ ) states that there is no significant difference between the means of the two methods being compared while the alternate hypothesis states that there is significant between the means of the two methods. Therefore, from the result, the null hypothesis was not rejected because there is weak evidence for the alternative hypothesis to be accepted.

Table 4.5. Two-tailed test for percentage difference between ASTM and TDCR methods

Difference	-1.839
T (Observed value)	-0.907
t  (Critical value)	2.042
Df	30
p-value (Two-tailed)	0.372
Alpha	0.05

Figure 4.1 shows the relationship between ASTM and TDCR methods employed in calculating the activity concentration of  $^{90}\text{Sr}$ . The figure shows the reliability of the TDCR method in determining the activity concentration of  $^{90}\text{Sr}$  in environmental samples. The numbers on the X-axis represent the name of the sampling locations (e.g., 16 represent Montevideo).

#### 4.4. Reproducibility evaluation

Table 4.6 shows the reproducibility results between the first samples and their duplicates both for the  $^{137}\text{Cs}$  and  $^{90}\text{Sr}$ . This statistical analysis verifies that the methods employed for analyses of the soil samples were reproducible.

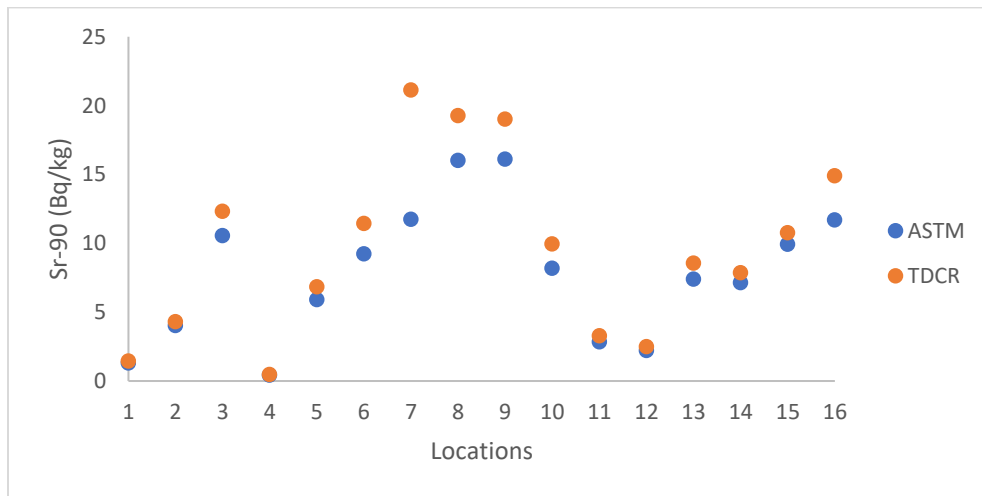


Figure 4.1. Relationship between the ASTM and TDCR methods in determining  $^{90}\text{Sr}$  activity

#### 4.5. Performance evaluation of reference materials

Table 4.7 provides the result of the MAPEP reference materials analyzed to validate the separation process. The reproducibility in the process appears to be acceptable when comparing the MAPEP-23-MaS48 and MAPEP-23-MaS48 DUP to their known activities. All analysis performed agreed with the known MAPEP values.

Table 4.6. Reproducibility test

Location	Split sample meeting criteria	Results
	$ A_1 - A_2  < 3(\sigma_1^2 + \sigma_2^2)^{1/2}$	Pass/Fail
Crystal Ice cave	1	Pass
Frenchman's cabin	1	Pass
Reno ranch	1	Pass

Table 4.7. Results of  $^{90}\text{Sr}$  in certified reference materials

Sample	Sample	ASTM	TDCR	ASTM	TDCR	$A_{ref}$	$A_{ref}$ (Bqkg <sup>-1</sup> )
	Counts	$A_{lab}$ (Bqkg <sup>-1</sup> )	$A_{lab}$ (Bqkg <sup>-1</sup> )	MDA (Bqkg <sup>-1</sup> )	MDA (Bqkg <sup>-1</sup> )	(Bqkg <sup>-1</sup> )	Acceptance Range
MAPEP- 23-MaS48 A	11440	812.78±57.43	811.14±57.24	18.25	18.16	920	644-1196
MAPEP- 23-MaS48 DUP	11992	851.52±60.12	854.53±60.27	18.25	18.16	920	644-1196
MAPEP- 27-MaS47	11371	824.66±58.27	807.70±57.02	18.33	18.24	852	596-1108

#### 4.5.1. Result validation by certified reference materials

Table 4.8 presents the summary of the performances of <sup>90</sup>Sr analysis activities in the environmental MAPEP reference samples. The evaluation results of bias of the certified reference materials varies from -0.10 to -0.03 and -0.09 to -0.05 in the ASTM and TDCR methods respectively. The evaluation results of the relative precision using the two methods were 0.07 for both reference samples analyzed while the accuracy (degree of agreement with the accepted reference value) is 0.16 and 0.17 using the ASTM and TDCR methods respectively. The performance of <sup>90</sup>Sr analysis results using the ASTM and TDCR methods also demonstrates the reliability of the two analytical methods.

Table 4.8. Performance evaluation of reference soil samples

<b>Sample</b>	<b>Bias</b> (-0.25-0.50)	<b>Relative Precision</b> (2% ≤ RP ≤ 15%)	<b>Accuracy</b> $ Bias  \leq \frac{A_m}{A_r} \times 2.58RP$	<b>Result</b> Pass/fail
<b>MAPEP-23-</b>				
<b>MaS48</b>				
ASTM	-0.10	0.07	0.16	Pass
TDCR	-0.09	0.07	0.16	Pass
<b>MAPEP-27-</b>				
<b>MaS47</b>				
ASTM	-0.03	0.07	0.17	Pass
TDCR	-0.05	0.07	0.17	Pass

Table 4.9 shows the ratio of  $^{137}\text{Cs}$  to  $^{90}\text{Sr}$  in the sampled soils using the two methods of calculation. The ratio of  $^{137}\text{Cs}$  to  $^{90}\text{Sr}$  in the sampled soils ranges from 0.33 to 40.88 and 0.27 to 35.87 using the ASTM and TDCR methods respectively. The average of  $^{137}\text{Cs}$  to  $^{90}\text{Sr}$  ratio are 4.29 and 3.73 using the ASTM and TDCR methods respectively. These values are somewhat higher than the global fallout ratio of 1.6 and 1.8. However, there is great variability in this ratio globally, and these ratio values, although greater than the mean values, are not unusual given the global variability. Furthermore, a one-sample t-test was performed to determine if the observed ratios significantly differ from the expected value. Table 4.10 presents the result of the one-sample t-test performed on the  $^{137}\text{Cs}$  to  $^{90}\text{Sr}$  ratio. The null hypothesis failed to be rejected as there is weak evidence for the alternative hypothesis to be accepted.

Figure 4.2 is a plot demonstrating trend relationships between the activity concentration of  $^{137}\text{Cs}$  and  $^{90}\text{Sr}$  for both ASTM and TDCR methods. Some locations such as Blackfoot, Butte city, Howe show how closely related the ratio of  $^{137}\text{Cs}$  to  $^{90}\text{Sr}$  are. The activity concentration of  $^{90}\text{Sr}$  for both ASTM and TDCR methods is higher than the  $^{137}\text{Cs}$  in FAA Tower and Frenchman's cabin.

Figure 4.3 shows the relationship between the ASTM and TDCR methods in determining  $^{137}\text{Cs}$  to  $^{90}\text{Sr}$  ratio in all the locations. This figure demonstrates the consistency between these two methods comparing the ratio of  $^{137}\text{Cs}$  to  $^{90}\text{Sr}$  in the soil samples.

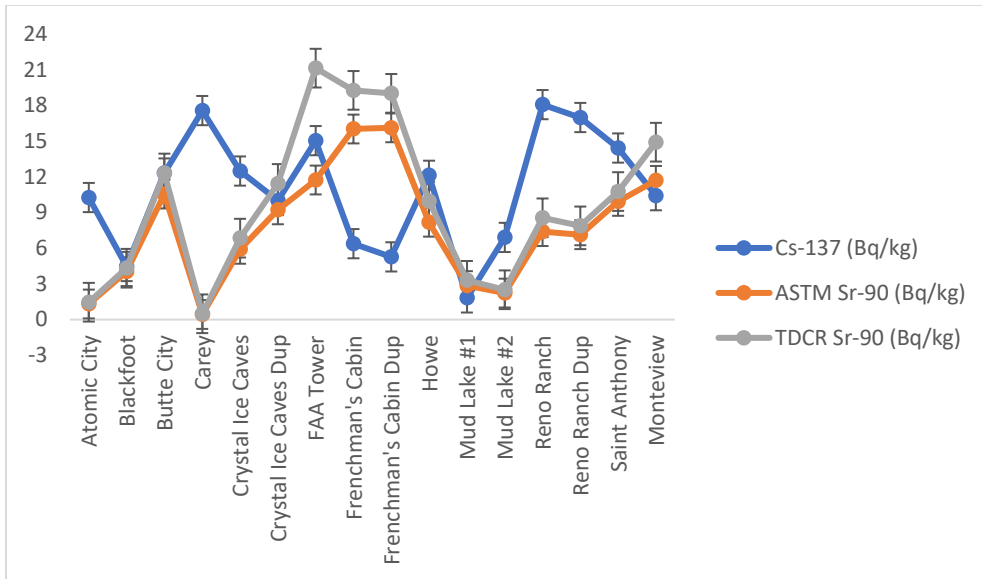


Figure 4.2. Relationship between  $^{137}\text{Cs}$  and  $^{90}\text{Sr}$  for both ASTM and TDCR methods

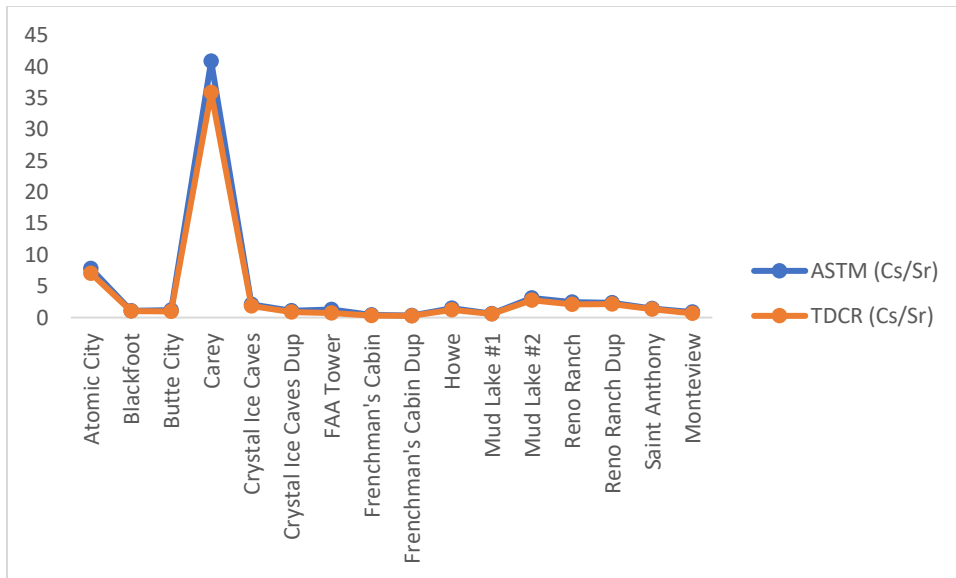


Figure 4.3. Relationship between  $^{137}\text{Cs}$  to  $^{90}\text{Sr}$  ratio in both ASTM and TDCR methods

Table 4.9. Radioactivity concentration in <sup>90</sup>Sr and <sup>137</sup>Cs in soil samples

<b>Radioactivity concentration (Bq/kg)</b>					
<b>Location</b>	<b>Cs-137</b>	<b>Sr-90</b>		<b>ASTM</b>	<b>TDCR</b>
		<b>ASTM</b>	<b>TDCR</b>	<b>Cs/Sr</b>	<b>Cs/Sr</b>
Atomic City	10.27±1.59	1.31±3.83	1.46±3.59	7.84	7.03
Blackfoot	4.46±1.23	4.03±3.78	4.32±3.55	1.11	1.03
Butte City	12.33±1.76	10.56±3.95	12.33±3.79	1.17	1.00
Carey	17.58±2.06	0.43±3.74	0.49±3.59	40.88	35.88
Crystal Ice cave	12.50±1.79	5.91±3.83	6.85±3.63	2.11	1.82
Crystal Ice cave	10.02±1.87	9.23±3.83	11.45±3.72	1.09	0.87
Dup					
FAA Tower	15.05±1.99	11.74±3.99	21.15±3.99	1.28	0.71
Frenchmen's Cabin	6.39±1.31	16.03±4.00	19.28±3.90	0.40	0.33
Frenchmen's Cabin Dup	5.27±1.28	16.13±4.15	19.03±3.95	0.33	0.28
Howe	12.14±1.69	8.19±3.85	9.97±3.73	1.48	1.22
Mud Lake #1	1.82±0.88	2.86±3.73	3.30±3.53	0.64	0.55
Mud Lake #2	6.91±1.30	2.23±3.68	2.51±3.52	3.10	2.75
Reno Ranch	18.08±2.12	7.40±3.99	8.56±3.69	2.44	2.11
Reno Ranch Dup	16.99±2.00	7.14±3.95	7.88±3.69	2.38	2.15
St. Anthony	14.43±1.82	9.94±4.30	10.77±3.72	1.45	1.34
Monteview	10.42±1.45	11.71±3.95	14.92±3.86	0.89	0.70
<b>Average</b>	<b>10.92±1.63</b>	<b>7.80±3.91</b>	<b>9.64±3.72</b>	<b>4.29</b>	<b>3.73</b>

Table 4.10. One-sample t-test of  $^{137}\text{Cs}$  to  $^{90}\text{Sr}$  ratio

<b>Parameters</b>	<b>ASTM</b>	<b>TDCR</b>
Mean	4.29	3.74
Std. dev.	9.917911	8.72182
SEM	2.479478	2.180455
Df	15	15
T	1.002983	0.887716
p-value	0.331775	0.388706

To test the difference between the ratio of  $^{137}\text{Cs}$  to  $^{90}\text{Sr}$  around the INL compared to areas farther away, a log transformation was carried out on the  $^{137}\text{Cs}$  to  $^{90}\text{Sr}$  ratio. Table 4.11 represents the summary of results of the transformed data. Figure 4.4 shows the box plot of the treatments, zero (0) representing areas not near INL while one (1) represents areas near INL. The p-value gives 0.07 which shows that a significant difference occurs between the  $^{137}\text{Cs}$  to  $^{90}\text{Sr}$  ratio around INL than areas farther away. Therefore, the alternative hypothesis failed to be rejected.

Table 4.11. Summary of transformed data

	<b>Df</b>	<b>Sum Sq.</b>	<b>Mean Sq.</b>	<b>F-value</b>	<b>p-value</b>
<b>Treatment</b>	1	4.427	4.427	3.75	0.07
<b>Residuals</b>	14	16.524	1.180		

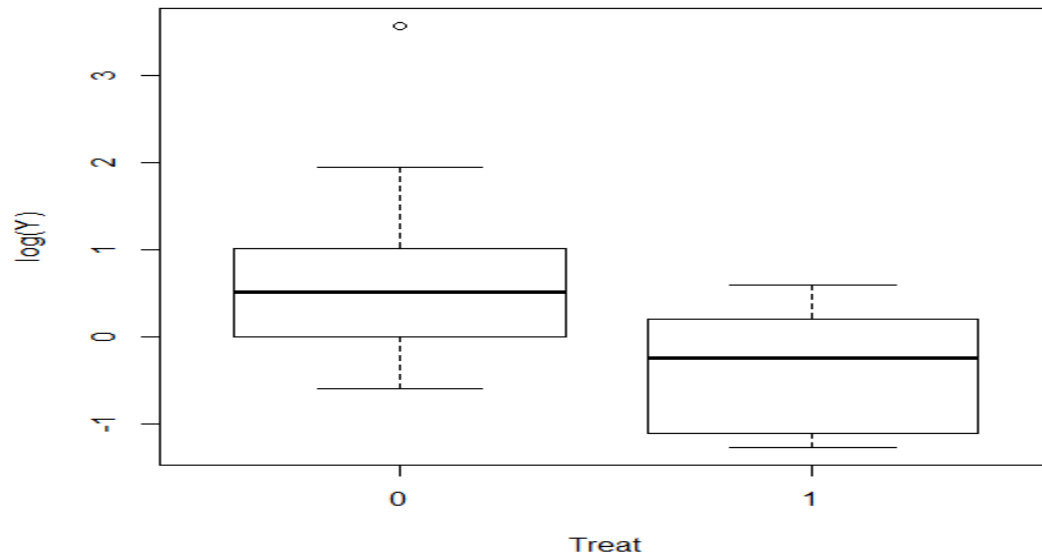


Figure 4:4. Box plot of treatments after log transformation

## Chapter 5 : Conclusion

### 5.1. Summary of results

The ratio of  $^{137}\text{Cs}$  to  $^{90}\text{Sr}$  in soils around INL has been investigated in this study. Extraction chromatography separation method was used to separate  $^{90}\text{Sr}$  in soil samples using Sr Resin. A recent technology called triple to double coincidence ratio (TDCR) counting method was used to analyze the concentration of  $^{90}\text{Sr}$  in the soil samples. The TDCR method was then compared with the traditional method (ASTM). The comparison of these two methods showed that there is no statistical difference between the means of these two methods. The chemical recovery correction of the measured activities showed good comparisons while the efficiency of the  $^{90}\text{Sr}$  standard was sufficiently high for the measurement process. The method validation by certified reference materials provided by MAPEP demonstrated good agreement between the measured activities and the acceptance range of activities given.

The activity concentration of  $^{137}\text{Cs}$  in the locations evaluated varies from  $10.92 \pm 1.63$  Bq/kg to  $18.08 \pm 2.12$  Bq/kg. All the measured values are less than the recommended federal screening limit for surface soil. The values observed for  $^{90}\text{Sr}$  activity concentration in the soil samples are between  $0.43 \pm 3.74$  to  $16.13 \pm 4.15$  Bq/kg and between  $0.49 \pm 3.59$  to  $21.15 \pm 3.99$  Bq/kg for the ASTM and TDCR methods respectively. Statistically, the duplicate sample data when compared with the main sample data shows the reproducibility of the separation process.

The hypothesis ( $H_{1,0}$ ) that the ratio of  $^{137}\text{Cs}$  to  $^{90}\text{Sr}$  in the sampled soils is equal to the expected value cannot be rejected as there is weak evidence for the alternative hypothesis to be accepted. As shown in Table 4.10, the p-value of one-sample t-test of  $^{137}\text{Cs}$  to  $^{90}\text{Sr}$  ratio supports the suggestion that the analyzed soil samples are equal to the global fallout ratio of 1.6 to 1.8.

The hypothesis ( $H_{2,a}$ ) that the ratio of  $^{137}\text{Cs}$  to  $^{90}\text{Sr}$  around the INL is higher than the ratio of  $^{137}\text{Cs}$  to  $^{90}\text{Sr}$  in other areas due to the activities of INL failed to be rejected. As shown in Table 4.11, after log transformation was carried out to test the difference between the ratio of  $^{137}\text{Cs}$  to  $^{90}\text{Sr}$  in soil samples around the INL compared to areas farther away, the result indicates that a significant difference occurs between the  $^{137}\text{Cs}$  to  $^{90}\text{Sr}$  ratio around INL than areas farther away. Considering the apriori rule of p value equal 0.05, it can be concluded that there is no clear evidence that the INL activities contribute to the  $^{90}\text{Sr}$  in areas around INL.

The hypothesis ( $H_{3,0}$ ) that there is no significant difference between the means of the traditional method (ASTM) used for determining  $^{90}\text{Sr}$  activity concentration and the TDCR method was not rejected. As shown in Table 4.5, the two-tailed test at the 95% confidence level for the comparisons indicates that the percentage difference is statistically insignificant. Therefore, from the result, the null hypothesis was not rejected because there was weak evidence for the alternative hypothesis to be accepted.

The extraction separation process using the Sr resin (50-100  $\mu\text{m}$ ) by Eichrom® to separate  $^{90}\text{Sr}$  from soil samples and subsequently analyzed on the Hidex 300 SL LSC proves to be an effective method.

## **5.2. Future work**

1. For the determination of  $^{90}\text{Sr}$ , a direct measurement should be carried out on the samples without the need for radiochemical separation process. This would allow for fast and inexpensive method of  $^{90}\text{Sr}$  analysis especially when dealing with an emergency response situation. However, this should be verified with measurement after radiochemical separation to know how effective the method performs.

2. Mass spectrometry system (either Accelerator Mass Spectrometry or Integrated Coupled Mass Spectrometry) can be used for the determination of  $^{85}\text{Sr}$  recovery and for the determination of  $^{90}\text{Sr}$  in soil samples.
3. More samples can be collected to give a clearer picture of the difference in the  $^{137}\text{Cs}$  to  $^{90}\text{Sr}$  ratio between the areas surrounding the INL and the areas farther away.

## References

- Ahmad AY, Al-Ghouti MA, AlSadig I, Abu-Dieyeh M. Vertical distribution and radiological assessment of  $^{137}\text{Cs}$  and natural radionuclides in soil samples. *Scientific Reports* 9 (12196); 2019. <https://doi.org/10.1038/s41598-019-48500-x>.
- Al-Masri MS. Cerenkov counting technique. *Journal of Radioanalytical and Nuclear Chemistry* 205: 205-213; 1996.
- Andrello AC, Appoloni CR. Spatial Variability and Cesium-137 Inventories in Native Forest. *Brazillian Journal of Physics* 34(3A): 800-803; 2004.
- ANSI, 1996. An American National Standard – Performance criteria for radiobioassay. Health Physics Society, Virginia, HPS N13.30; 1996.
- Asgharizadeh F, Salimi B, Marageh MG, Mahani MK, Aliabadi M. Determination of  $^{90}\text{Sr}$  concentration in soil and sediment samples from southern shores of Iran using a Sr resin and LSc method. *Adv. Liq. Scintill. Spectrom.* 299-303; 2009.
- ASTM C1507-07. Standard test method for radiochemical determination of strontium-90 in soil. ASTM International, West Conshohocken, PA. 2009.
- Ball JE. Deposition of strontium-90 in soil and vegetation at various locations surrounding the Fukushima daiichi nuclear power plant. Thesis submitted to Colorado State University. Pp. 37; 2015.
- Bondar YI, Navumau AD, Nikitin AN, Brown J, Dowdall M. Model assessment of additional contamination of water bodies as a result of wildfires in the Chernobyl exclusion zone. *Journal of Environmental Radioactivity* 138: 170-176; 2014.

- Bosworth LM. A comparison of  $^{137}\text{Cs}$  in sage brush wood (*Artemisia tridentata*) with historical release data from the Idaho Chemical Processing Plant located on the Idaho National Engineering Laboratory site. Thesis submitted to Idaho State University. Pp. 49; 1995.
- Brennan C, Haas D, Landsberger S, Artnak E, Bator G, Bednar A, Kovacs T. A feasibility study on the determination of  $^{90}\text{Sr}$  food-chain transfer using stable strontium as a surrogate and neutron activation analysis. *Journal of Environmental Radioactivity* 208-209 (105988); 2019.
- Buchanan R. SC&A'S evaluation of Cs-137/Sr-90, fission and activation product, and actinide values using ANL-W monthly and annual waste reports in relationship to assigning intakes. National Institute for Occupational Safety and Health. Contract No. 211-2014-58081 SCA-TR-2017-SEC002, Revision 0.
- Burger A, Lichtscheidl I. Strontium in the environment: Review about reactions of plants towards stable and radioactive strontium isotopes. *Science of the Total Environment* 653: 1458-1512; 2019.
- Buchtela K. Radiochemical Methods Gamma-Ray Spectrometry. Editor(s): Paul Worsfold, Colin Poole, Alan Townshend, Manuel Miró, *Encyclopedia of Analytical Science* (Third Edition), Academic Press 15-22; 2019. <https://doi.org/10.1016/B978-0-12-409547-2.11333-2>.
- Cao Y, Zhao Z, Wang P. *et al.* 2021. Long-term variation of  $^{90}\text{Sr}$  and  $^{137}\text{Cs}$  in environmental and food samples around Qinshan nuclear power plant, China. *Scientific Reports* 11 (20903); 2021. <https://doi.org/10.1038/s41598-021-00114-y>.

- Carvalho FP, Oliveira JM, Malta M. Forest fires and resuspension of radionuclides into the atmosphere. *American Journal of Environmental Sciences* 8 (1): 1-4; 2012.
- Carvalho FP, Oliveira JM, Malta M. Exposure to radionuclides in smoke from vegetation fires. *Science of the Total Environment*. 472: 421-424; 2014.
- Chaligava O, Grozdov D, Yushin N. *et al.* Distribution of natural and anthropogenic radionuclides in soil samples in recreational zones of Moscow. *Water Air Soil Pollution*. 233 (448); 2022. <https://doi.org/10.1007/s11270-022-05930-0>.
- Corcho-Alvarado JA, Balsiger B, Sahil H, Astner M, Byrde F, Rollin S, Holzer R, Mosimann N, Wuthrich S, Jakob A, Burger M. Long-term behavior of (90) Sr and (137) Cs in the environment: Case studies in Switzerland. *Journal of Environmental Radioactivity* 160 (54-63); 2016.
- Craig PP, Jungerman JA, Krass A. Nuclear arms race: technology and society. *American Journal of Physics* 54 (765): 1986. doi: 10.1119/1.14460.
- Curie LA. Limits for qualitative detection and quantitative determination, application to radiochemistry. *Anal Chem* 40: 586-593; 1968.
- Dai X, Cui Y, Kramer-Tremblay S. A rapid method for determining strontium-90 in urine samples. *J. Radioanal. Nucl. Chem*. 296: 363-368; 2013.
- Done L, Loan MR. Minimum detectable activity in gamma spectrometry and its use in low level activity measurements. *Appl. Radiat. Isot.* 114: 28-32; 2016.
- Eichrom. Sr Resin. Accessed on March 20, 2023, from [Sr Resin - Eichrom Technologies Inc.](#)

- Eisenbud M, Gesell T. Environmental radioactivity from natural, industrial, and military sources. fourth ed. Academic Press, San Diego, CA; 1997.
- Environmental Protection Agency (EPA). Guidance on systematic planning using the data quality objectives process, EPA QA/G-4. Office of Environmental Information Washington, DC 20460. EPA/240/B-06/001; 2006.
- Falkner JT. Minimum detectable activity as a function of detector speed. Doctoral dissertation, Texas A&M University. Pp.121; 2018.
- González-Delgado AM, Thakur P. Effect of soil properties on radioactivity concentrations and dose assessment. *Journal of Radioanalytical and Nuclear Chemistry* 331: 3535-3544; 2022.
- Grahek Z, Dulanska S, Karanovic G, Coha I, Tucakovic I, Nodilo M, Matel L. Comparison of different methodologies for the  $^{90}\text{Sr}$  determination in environmental samples. *Journal of Environmental Radioactivity* 181: 18-31; 2018.
- Gustafson PF. Ratio of Cesium-137 and Strontium-90 radioactivity in soil. *Science* 130(3386): 1414-1415; 957.
- Hamzah Z, Saat A, Riduan SD, Amirudin CY. Assessment of  $^{137}\text{Cs}$  activity concentration in soil from tea plantation areas in Cameron Highlands. *Journal of Nuclear and Related Technologies* 9(1): 1-5; 2012.
- Hasan AK, Askouri NA, Talib HM. Calculation of the amounts of fission products ( $^{85}\text{Kr}$ ,  $^{129}\text{I}$ ,  $^{137}\text{Cs}$ ) in pressurized water reactors (PWR). *International Journal of Science and Research* 3(11): 334-337; 2014.

- Herranz M, Romero LM, Idoeta R, Olondo C, Valino F, Legarda F. Inventory and vertical migration of  $^{90}\text{Sr}$  fallout and  $^{137}\text{Cs}/^{90}\text{Sr}$  ratio in Spanish mainland soils. *Journal of Environmental Radioactivity* 102: 987-994; 2011.
- Horwitz PE, Dietz ML, Chiarizia R. A novel strontium-selective extraction chromatographic resin. *Solv. Extr. Ion Exch.* 10(2): 313–336; 1992. <https://doi.org/10.1080/07366299208918107>.
- Hou, X. Liquid scintillation counting for determination of radionuclides in environmental and nuclear application. *J Radioanal Nucl Chem* 318: 1597–1628; 2018.
- Hou X, Dai X. Environmental liquid scintillation analysis. *Handbook of Radioactivity Analysis Volume 2*: 41-136; 2020.
- Idaho National Laboratory (INL). Historical Data Analysis Supporting the Data Quality Objectives for the INL Site Environmental Soil Monitoring Program. February 2017. INL/INT-15-37431 Revision 0.
- INL ESER (Environmental Surveillance, Education and Research). 2020. Accessed via wildland fire ([inl.gov](http://inl.gov)) on 20th September 2022.
- International Organization for Standardization (ISO). Uncertainty of measurement Part 3: Guide to the expression of uncertainty in measurement (GUM: 1995). ISO/IEC Guide 98-3:2008.
- International Organization for Standardization (ISO). Measurement of radioactivity in the environment – soil – Part 5: Strontium 90 – Test method using proportional counting or liquid scintillation counting. ISO 18589-5:2019.
- Kim G, Lee DS, Eccles H, Kim SM, Cho HU, Park JM. Selective strontium adsorption using synthesized sodium titanate in aqueous solution. *RSC Advances* 12: 18936-18944; 2022.

- Kirkpatrick JM, Venkataraman R, Young BM. Minimum detectable activity, systematic uncertainties, and the ISO 11929 standard. *J Radioanal Nucl Chem.* 296: 1005-1010; 2013.
- Lee HY, Kim W, Kim Y, Maeng S, Lee SH. Activity concentration of  $^{137}\text{Cs}$  and  $^{90}\text{Sr}$  in seawaters of East Sea, Korea. *Journal of Radiation Protection and Research* 41(3): 268-273; 2016.
- Lopes I, Mourato A, Abrantes J, Carvalhal G, Madruga MJ, Reis M. Quality control assurance of strontium-90 in foodstuffs by LSC. *Applied Radiation and Isotopes. Appl. Radiat. Isot.* 93: 29-32; 2014.
- Marchesani G, Trotta G, De Felice P, Bortone N, Damiano R, Nicolini M, Accettulli R, Chiaravalle AE, Lammarino M. Fast and Sensitive Radiochemical Method for Sr-90 Determination in Food and Feed by Chromatographic Extraction and Liquid Scintillation Counting. *Food Anal. Methods* 15: 1521–1534; 2022. <https://doi.org/10.1007/s12161-021-02191-1>.
- Maxwell SL, Culligan BK, Shaw PJ. Rapid determination of radiostrontium in large soil samples. *Journal of Radioanalytical and Nuclear Chemistry* 295: 965–971; 2013. <https://doi.org/10.1007/s10967-012-1863-2>.
- Mehmood K. Environmental behavior of cesium and strontium in agricultural and forest soil. Dissertation, der Rheinischen Friedrich-Wilhelms-Universität Bonn. Pp 87: 2018.
- Miki S, Fujimoto K, Shigenobu Y, Ambe D, Kaeriyama H, Takagi K, Ono T, Watanabe T, Sugisaki H, Morita T. Concentrations of  $^{90}\text{Sr}$  and  $^{137}\text{Cs}/^{90}\text{Sr}$  activity ratios in marine fishes after the Fukushima Dai-ichi Nuclear Power Plant accident. *Fish. Oceanogr.* 26(2): 221-233; 2017.

Muck K, Sinojmeri M, Steger F. Long-term availability of Sr-90 in foodstuff after nuclear fallout. Austrian Research Center Seibersdorf, A-2444 Seibersdorf. Environmental Science P-11-246; 2000.

Murray RL. Understanding Radioactive Waste. 5th Ed. Battelle Press, Columbus, OH; 2003.

National Center for Biotechnology Information (NCBI). PubChem Compound Summary for CID 5486204, Strontium-90. Accessed March 17, 2023, from <https://pubchem.ncbi.nlm.nih.gov/compound/Strontium-90>.

National Council on Radiation Protection and Measurements (NCRP). Recommended Screening Limits for Contaminated Surface Soil and Review of Factors Relevant to Site-Specific Studies. NCRP Report No. 129. Bethesda, MD. 1999.

Nguyen T, Tran Q, Nguyen V, Le N, Phan S, Le X, Vuong T, Nguyen V, Nguyen D, Tran D, Nguyen M, Phan Q, Vo T, Duong V, Le N. Activity concentrations of Sr-90 and Cs-137 in seawater and sediment in the gulf of Tonkin, Vietnam. Hindawi Journal of Chemistry 8752606 (8); 2020.

Penrose B, Beresford NA, Broadley MR, Crout NMJ. Inter-varietal variation in caesium and strontium uptake by plants: a meta-analysis. Journal of Environmental Radioactivity 139, 103-117; 2015. <https://doi.org/10.1016/j.jenvrad.2014.10.005>.

L'Annunziata MF. Handbook of Radioactivity Analysis (Second Edition). Elsevier; 2004.

Rivera-Silva J, Hurtado-Bermudez S, Villa-Alfageme M, Manjon G. Comparison and validation of methods for the determination of <sup>90</sup>Sr by Cerenkov counting in biological and sediment samples, including green chemistry metrics. J Radioanal Nucl Chem 320:109–122; 2019.

- Russell BC, Croudace IW, Warwick PE. Determination of  $^{135}\text{Cs}$  and  $^{137}\text{Cs}$  in environmental samples: A review. *Analytica Chimica Acta*, 890: 7-20; 2015  
<https://doi.org/10.1016/j.aca.2015.06.037>.
- Sahoo S, Kavasi N, Sorimachi A, Arae H, Tokonami S, Mietelski JW, Lokas E, Yoshida S. Strontium-90 activity concentration in soil samples from the exclusion zone of the Fukushima daiichi nuclear power plant. *Sci Rep* 6 (23925); 2016.
- Sarap NB, Jankovic MM, Dolijanovic ZK, Kovacevic DD, Rajacic MM, Nikolic JD, Todorovic DJ. Soil-to-plant transfer factor for  $^{90}\text{Sr}$  and  $^{137}\text{Cs}$ . *J Radioanal Nucl Chem* 303: 2523-2527; 2014.
- Shao Y, Yang, G, Tazoe H, Ma L, Yamada M, Xu D. A review of measurement methodologies and their applications to environmental  $^{90}\text{Sr}$ . *Journal of Environmental Radioactivity* 192: 321-333; 2018.
- Sharma S. Uptake, transport, and remediation of strontium. *The Handbook of Environmental Chemistry* 88: 99-119; 2020.
- Sherrill RD, Sumerlin NG, Beck JN, Kuroda PK. Variation of the ratio of Cesium-137 to Strontium-90 in the atmosphere. *Health Physics* 28: 335-340; 1975.
- Simon SI, Bouville A, Moroz B, Beck H. Long-term consequences of radioactive fallout from conflicts involving nuclear explosions. *American Geophysical Union Fall Meeting San Frasco, CA*, 2016.
- Smith J. 2018. Evaluation of Cs-137 global fallout in soils at Fort Calhoun Station. FC-18-003 Revision 1: 1-15; 2018.

- Solatie D, Carbol P, Hmecek E, Jaakkola T, Betti M. Sample preparation methods for the determination of plutonium and strontium in environmental samples by low level liquid scintillation counting and  $\alpha$ -spectrometry. *Radiochim. Acta* 90: 447-454; 2002.
- Tayeb M, Dai X, Corcoran EC, Kelly DG. Evaluation of interferences on measurements of  $^{90}\text{Sr}/^{90}\text{Y}$  by TDCR Cherenkov counting technique. *J Radioanal Nucl Chem* 300: 409-414; 2014.
- Tayeb M. Development of rapid methodologies for the determination of strontium-90 in water using triple-to-double coincidence ratio (TDCR) Cerenkov counting and liquid scintillation assay techniques. Thesis submitted to the Division of Graduate Studies of the Royal Military College of Canada. Pp.198; 2015.
- Torres JM, Tent J, Llauro M, Rauret G. A rapid method for  $^{90}\text{Sr}$  determination in the presence of  $^{137}\text{Cs}$  in environmental samples. *Journal of Environmental Radioactivity* 59: 113-125; 2002.
- United States Nuclear Regulatory Commission (USNRC). Radiological environmental monitoring program. Inspection Procedure 71124 Attachment 07; 2020.
- Vajda N, Kim, C-K. Determination of radiostrontium isotopes: a review of analytical methodology. *Appl. Radiat. Isot.* 68: 2306-2326; 2010.
- VanHorn R, Harney T. Long-Term Ecological Monitoring Plan for the Idaho National Laboratory. Idaho Cleanup Project Idaho Falls, Idaho 83415. Prepared for the U.S. Department of Energy Assistant Secretary for Environmental Management Under DOE/NE Idaho Operations Office. 2007.

Wang J. A quick liquid scintillation counting technique for analysis of  $^{90}\text{Sr}$  in environmental samples. *Applied Radiation and Isotope* 81: 169-174; 2013.

Yang Y, Zhang H, Wang Y, Ma Y, Dai X, Ai Y, Huang Y. Influence of various parameters on TDCR Cerenkov counting technique. *Journal Radioanalytical and Nuclear Chemistry* 329: 499–509; 2021.

Zhou Z, Ren H, Zhou L, Wang P, Lou X, Zou H, Cao Y. Recent development on determination of low-level  $^{90}\text{Sr}$  in environmental and biological samples: A review. *Molecules* 28: 90; 2022.

Zhu Y, Smolders E. Plant uptake of radiocesium: a review of mechanisms, regulation and application. *J. Exp. Bot.* 51: 1635–1645; 2000.

Appendix A. <sup>85</sup>Sr certificate of calibration



Eckert & Ziegler

Isotope Products

24937 Avenue Tibbitts  
Valencia, California 91355

Tel 661 309 1010  
Fax 661 257 8303

RS58984

CERTIFICATE OF CALIBRATION  
GAMMA STANDARD SOLUTION

<b>Radionuclide:</b> Sr-85	<b>Customer:</b> IDAHO STATE UNIVERSITY
<b>Half-life:</b> 64.849 ± 0.004 days	<b>P.O. No.:</b> P0040702
<b>Catalog No.:</b> 7085	<b>Reference Date:</b> 1-Aug-23 12:00 PST
<b>Source No.:</b> 2378-96	<b>Contained Radioactivity:</b> 10.98 nCi 406.3 Bq

Physical Description:

A. Mass of solution:	125.0943 g in 125 mL bottle
B. Chemical form:	SrCl <sub>2</sub> in 0.5M HCl
C. Carrier content:	50 µg Sr/mL of solution
D. Density:	1.0077 g/mL @ 20°C

Radioimpurities:

None detected

Radionuclide Concentration: 0.08777 nCi/g, 3.247 Bq/g

Method of Calibration:

This source was prepared from a weighed aliquot of solution whose activity in µCi/g was determined using a pressurized well type ionization chamber.

Uncertainty of Measurement:

A. Type A (random) uncertainty:	± 0.1 %
B. Type B (systematic) uncertainty:	± 3.0 %
C. Uncertainty in aliquot weighing:	± 0.6 %
D. Total uncertainty at the 99% confidence level:	± 3.1 %

Notes:

- See reverse side for leak test(s) performed on this source.
- EZIP participates in a NIST measurement assurance program to establish and maintain implicit traceability for a number of nuclides, based on the blind assay (and later NIST certification) of Standard Reference Materials (as in NRC Regulatory Guide 4.15).
- Nuclear data was taken from IAEA-TECDOC-619, 1991.
- This solution has a recommended working life of 4 months.

S. Pournelo  
Quality Control

26 Jun 23  
Date

EZIP Ref. No.: 2378-96

ISO 9001 CERTIFIED

Medical Imaging Laboratory  
24937 Avenue Tibbitts Valencia, California 91355

Industrial Gauging Laboratory  
1800 North Keystone Street Burbank, California 91504

## Appendix B. Counting efficiency of $^{85}\text{Sr}$ source

15 ml of  $^{85}\text{Sr}$  was prepared and counted for 1800 seconds on ORTEC gamma detector to determine the standard efficiency which was eventually used for chemical recovery determination in the samples. The net peak area was obtained and used to determine the counting efficiency of the 514 keV gamma ray of  $^{85}\text{Sr}$ .

Total counts = 1275

Count rate =  $1275/1800 = 0.71$  c/s

Count date = 09/12/23

Sr-85 reference date = 08/01/2023

Date between reference date and count date,  $t = 42$  days = 3628800 s

Decay correct activity,  $A = A_0 e^{-\lambda t}$

Half-life of Sr-85 = 65 days = 5616000 s

$$\lambda = \frac{0.693}{5616000} = 1.23 \times 10^{-7} \text{ s}^{-1}$$

$A = 31.17$  Bq

$$\text{Efficiency} = \frac{\text{Count rate}}{\text{Activity}} \times \gamma$$

Where  $\gamma$  is Sr-85 gamma yield (0.99280)

Efficiency = 0.0226

## Appendix C: Preparation of reagents

### Preparation of 3 M HNO<sub>3</sub> - 0.05 M Oxalic acid

1. Add 190 ml of concentrated HNO<sub>3</sub> (15.8 M) and 6.3 grams of oxalic acid dihydrate (C<sub>2</sub>H<sub>2</sub>O<sub>4</sub>·2H<sub>2</sub>O) to 800 ml of deionized water.
2. Dilute to 1 L of deionized water.

### Preparation of 8 M HNO<sub>3</sub>

1. In a 1-L volumetric flask, add 400 ml deionized water.
2. Add 506 ml concentrated HNO<sub>3</sub>.
3. Dilute to 1-L with deionized water.

### Preparation of 0.05 M HNO<sub>3</sub>

1. In a 1-L volumetric flask, add 900 ml deionized water.
2. Pipette 3.2 ml concentrated HNO<sub>3</sub>.
3. Dilute to 1-L with deionized water.

### Preparation of 20 mg/ml Sr(NO<sub>3</sub>)<sub>2</sub>

1. Dissolve 5 g of Sr(NO<sub>3</sub>)<sub>2</sub> in 50 ml of deionized water.
2. Dilute to 250 ml with deionized water.

## Appendix D. <sup>90</sup>Sr efficiency measurement report

### MEASUREMENT REPORT

Model title: sr90 efftest  
 Model version: 1.0  
 Model file: sr90efftemp.gum (2023-10-03)  
 Model S/W version: 0.99.10  
 Uncertainty coverage factor  $k = 1$

### REPORTED VARIABLES

*radionuclide*: sr-90  
                   = sr-90  
*date\_certified*: dil conc ref date  
                   = 2013-11-03 12:00:00.000 EST  
           *today*: date to correct for decay  
                   = 2023-09-21 12:00:00.000 EST  
*cert\_std*: eal sr90 solution (unc sum of vareience method)  
           = (143.900 ± 0.981) Bq/mL  
           *V1*: volume of 1st del solution  
               = (5.000 00 ± 0.005 77) mL  
           *V2*: second del of standard  
               = (3.000 00 ± 0.005 77) mL  
           *Tc*: time of count  
               = 3600 s  
*Sample*: sample count  
           = (3.065 39 ± 0.001 75) × 10<sup>6</sup>  
           *bkg*: bkg counts in interval  
               = 1759.0 ± 41.9  
*workingstd*: efficiency  
               = 0.937.70 ± 0.006 51

### UNCERTAINTY BUDGETS

Uncertainty Components for *workingstd*

<i>i</i>	<i>X<sub>i</sub></i>	<i>u<sub>i</sub>(y)</i>	% of variance
1	<i>cert_std</i>	0.0064	96.5 %
2	<i>V1</i>	0.000677	1.08 %
3	<i>V2</i>	0.000677	1.08 %
4	<i>T<sub>1/2</sub></i> ( <sup>90</sup> Sr)	0.000542	0.693 %
5	<i>Sample</i>	0.000536	0.677 %
6	<i>bkg</i>	1.28 × 10 <sup>-5</sup>	0.000 %

## Appendix E1. MAPEP reference sample

MAPEP-22-MaS47 Combined Report

Radiological						Units: (Bq/kg)		
Analyte	Result	Ref Value	Flag	Notes	Bias (%)	Acceptance Range	Unc Value	Unc Flag
Strontium-90	NR	852				596 - 1108		
Technetium-99	NR	1000				700 - 1300		
Thorium-228	NR	49				34 - 64		
Thorium-230	NR	43				30 - 56		
Thorium-232	NR	47				33 - 61		
Uranium-234	NR	50.8				35.6 - 66.0		
Uranium-238	NR	157				110 - 204		
Zinc-65	1133.9	1140	A		-0.5	798 - 1482	46.9	A

*Radiological Reference Date: August 1, 2022*

**Results Flags:**

- A = Result acceptable..... |Bias| <= 20%
- W = Result acceptable with warning..... 20% < |Bias| <= 30%
- N = Result not acceptable..... |Bias| > 30%
- RW = Report Warning
- NR = Not Reported

**Uncertainty Flags:**

- NOT ACCEPTABLE.....RP < 2%
  - ACCEPTABLE.....2% <= RP <= 15%
  - ACCEPTABLE WITH WARNING.....15% < RP <= 30%
  - NOT ACCEPTABLE.....RP > 30%
- Relative Precision (RP) = (Reported Uncertainty / Reported Result) x 100

**Notes:**

- (1) = False Positive
- (4) = Sensitivity Evaluation
- (5) = Total Metal
- (6) = Not Evaluated
- (11) = False Positive Test, Result Not Reported
- (17) = NOT DETECTED - reported a statistically zero result
- (25) = Result not reported with other gamma results
- (28) = Not Reporting Previously Reported Analyte

## Appendix E2. MAPEP reference sample

MAPEP-23-MaS48 Combined Report



Department of Energy RESL - 1955 Fremont Ave, MS4149 - Idaho Falls, ID 83415

*Laboratory Results For MAPEP-23-MaS48*  
(ISUE01) ISU Environmental Monitoring Laboratory  
785 5th 8th Ave Rm B107  
Pocatello, Idaho 83209

Inorganic							Units: (mg/kg)	
Analyte	Result	Ref Value	Flag	Notes	Bias (%)	Acceptance Range	Unc Value	Unc Flag
Antimony	NR	6.4				4.5 - 8.3		
Arsenic	NR	8.4				5.9 - 10.9		
Barium	NR	300				210 - 390		
Beryllium	NR	18.3				12.8 - 23.8		
Cadmium	NR	3.53				2.47 - 4.59		
Chromium	NR	43.4				30.4 - 56.4		
Cobalt	NR	39.4				27.6 - 51.2		
Copper	NR	83.9				58.7 - 109.1		
Lead	NR	20.5				14.4 - 26.7		
Mercury	NR	0.0174				Sensitivity Evaluation		
Nickel	NR	84.5				59.2 - 109.9		
Selenium	NR	5.76				4.03 - 7.49		
Silver	NR	19.6				13.7 - 25.5		
Technetium-99	NR	0.00174				0.00122 - 0.00226		
Thallium	NR	0.19				Sensitivity Evaluation		
Uranium-235	NR	0.055				0.039 - 0.072		
Uranium-238	NR	20.8				14.6 - 27.0		
Uranium-Total	NR	20.8				14.6 - 27.0		
Vanadium	NR	85				60 - 111		
Zinc	NR	96				67 - 125		

Radiological							Units: (Bq/kg)	
Analyte	Result	Ref Value	Flag	Notes	Bias (%)	Acceptance Range	Unc Value	Unc Flag
Americium-241	NR	0.9				Sensitivity Evaluation		
Cesium-134	3.1		A			False Positive Test	1.4	
Cesium-137	0.77		A			False Positive Test	1.26	
Cobalt-57	681.1	698	A		-2.4	489 - 907	48.6	A
Cobalt-60	732.9	795	A		-7.8	557 - 1034	20.9	A
Iron-55	NR					False Positive Test		
Manganese-54	1224.8	1230	A		-0.4	861 - 1599	62.7	A
Nickel-63	NR	1130				791 - 1469		
Plutonium-238	NR	0.52				Sensitivity Evaluation		
Plutonium-239/240	NR	101				71 - 131		
Potassium-40	535.3	574	A		-6.7	402 - 746	26.3	A
Strontium-90	NR	920				644 - 1196		

Issued 6/14/2023

Printed 8/7/2023